We thank both referees for their thoughtful and thorough reviews of our paper. We appreciate you taking the time to complete these reviews and welcome your helpful comments. We have revised the manuscript to address your review comments (see below). Throughout this response to review document your (referee review) comments are provided in regular, non-italic font text, our response comments are provided in red font (as here).

**Reviewer 1**

This study is an advance in modeling ice-rise evolution and sets a new state-of-the-art from which to understand more. The modeling work is clearly a strong contribution and it is interesting to contrast the response of the ice-rise divide to surface mass balance and to oceanic forcing. My overall reaction is that a stated goal of advancing modeling capabilities was to be able to interpret ice-rise stratigraphy as a function of the history of forcing (based on the abstract and introduction). The modeling shows many cases that indicate how forcing may be imprinted on the ice rise, but doesn't focus directly on the stratigraphy. The discussion mentions general features of the Raymond stack in relation to these calculations but doesn't address how specific histories may be inferred, and even if that goal is now accessible because of this type of advance in modeling or if data limitations are still significant. In particular, I couldn't connect all the results about divide migration to the overall goal of inferring past forcing and the resulting ice-rise evolution (including divide migration) without relating what is possible and what has been recorded through the stratigraphy. If the main point is how much the divide and triple junction may migrate at all, then the motivation could be reworked to emphasize that the timing and magnitude of migration is something that we need to know, maybe just even for the overall evolution and stability of ice rises less than the imprint on stratigraphy and how that history may be inferred in future work.

The conclusions seem to summarize best the main takeaways and it would help if the abstract, introduction, and figures better guide the reader through all of the model results in a more cohesive way to showcase these key points.

We agree that we don't focus on the stratigraphy. The goal of the paper is three-fold. First, do perturbations in SMB and ocean forcing lead to different divide migration rates? Second, if so, can we infer possible unique Raymond Arch geometries that can be interpreted as past changes in SMB or ocean forcing? Third, is the magnitude of divide migration controlled by the magnitude of the perturbation alone or is it controlled by other factors such as the bed topography?

To highlight these points in the paper, we have rewritten the abstract to make clear that we are really investigating changes in ice-rise divide position in response to SMB and shelf thickness perturbations. Moreover, we have removed redundant internal stratigraphy material from the introduction and sharpened the focus towards divide migration. We have updated the discussion section to underline that this work is a first step towards being able to interpret Raymond stacks with regard to their main forcing mechanism. While we are confident that abandoned stacks most likely indicate a SMB signal, the situation is more complicated for tilted stacks where shelf thickness and SMB perturbations are equally likely trigger mechanisms.

Also, if this type of work on triple junctions is completely new then I would highlight that more. I think that it is because 3D models have not been applied like this to ice rises before – so, what do these results mean for 2D interpretations? Are triple junctions commonly observed on ice rises?
Yes, it is new for a real world geometry. The main point which we now mention more clearly in the introduction is that some observed radar features (e.g. relic Raymond stack in the ice rise flank) could not be explained, but have been hypothesized to be linked to a merging/splitting of triple junctions. However, our simulations were not tailored towards investigating this and the applied perturbations are therefore not strong enough to give a definitive answer. Nonetheless, we have expanded and rewritten the introduction, discussion, and conclusion section to underline this particular point of the paper.

I think the conclusions and outcomes of this work would be stronger if the authors can better bridge between what has been done here, and where this can go interpreting ice-rise data and/or understanding ice-rise evolution in general. As a step towards making this point more clear in the text, it may be necessary to rework figures and/or text so that these main messages are clear and that the information shown in the figures is understood to be supporting a particular overall result (or results), as well as displaying specific calculations. As it is now there are a lot of specifics presented and it is hard for the reader to know the best way to use all of the results outside of this work. But, it is clear that the work is a strong contribution and hopefully this feedback can help to strengthen the presentation and therefore the impact of these results within the wider community.
As mentioned above, we have sharpened the abstract, introduction, discussion, and conclusions sections for better guidance of the reader to the main outcomes. We have also changed multiple Figures and deleted redundant material as suggested by reviewer 2.

Specific comments:

Pg. 1, Line 4: “other archives are missing” – if space, I’d be more specific about what archives you are referring to that are currently unavailable
We added “…such as rock outcrops …”

Pg. 1, Line 18: Clarify that ice rises are independent of the main ice sheet but what seems important here is that they are isolated from the ice shelf
We added “…is independent of the main ice sheet and the surrounding ice shelves…”

Pg. 2, Line 18: Suggest rephrasing “It appears higher Glen flow indices than n>3” since that is redundant and not as directly written as could be
This paragraph has been removed as we are not focusing on arch amplitude matching.

Figure 1: Seems like it would be more clear in the figure to use smaller dots to represent ice-rise locations
We have made them the dots a smaller. However, the purpose of this Figure is to show that ice rises are widespread all across the continent.

Figure 2: Type that is in dark-colored brown parts of the figure cannot be seen very well. I printed in black and white and it is unreadable. It is a matter of preference, but I think it helps the reader to have a), b), c) listed before you say what they show, rather than after.
We have made the brown fields lighter. As it is a personal preference, we would like to keep the a), b), c) ordering as is.

I'd be clear in what you are showing for perturbed cases in Figure 2 that these are isochrones and geometry for new steady state subject to these perturbed conditions. Would be worth more fully referring to Figure 2 in the text, as it isn't completely clear how much of a cartoon this is vs. an illustration of the two cases you'll try
We have updated the Figure caption to make this clearer (see Reviewer 2 comment). We now refer in 5 different places in the text to Figure 2.

Pg. 4, Line 11: Are these ice shelves larger than typically found or can you qualify "large" here for better context?
We added here: "…15th and 16th largest in Antarctica (Matsuoka et al., 2015)". Area numbers are listed in the study area section.

Pg. 4, Line 15: in this question does it have to be "or", could it be "and" among all three controls that you mention?
Yes, it could. We changed to and/or

Pg. 4, Line 24: I'm not sure what is meant by "...belong to the larger ice rises in Antarctica. . ." – but here is where you give context to size in relation to other ice rises, maybe worth mentioning earlier?
Done. See comment above.

Equation 1: Isn't there a minus sign missing?
Yes, of course. Thanks for spotting this.

Pg. 6, Line 7: Is there a physical meaning to the tuning parameters that can be shared simply here without having to go back to Favier et al. (2016)?
We added: "…G, and A are tuning parameters to constrain melt rates at the grounding line and away from the grounding line respectively, and α is a local tuning parameter (Table 1)."

Pg. 7, Line 16: Check formatting of ; and )
Done

Pg. 7, Line 23: Need to fix so that subscripts are for both B and C for each parameter
Fixed.

Pg. 7, Line 25: I'm not sure that I'd call L-curve analysis a way to "calibrate" the regularization parameters, really it is a way to pick them following a set of assumptions
Changed.

Pg. 8, Line 2: What do you mean by "data inconsistencies"?
We added: "… such as differences introduced by differing acquisition dates of ice surface elevation and surface velocity."

Also, would be good to clarify that the simulation length you are referring to is the relaxation simulation (10 years), as in the table you show 1000 years
Added.

Figure 3: Axes labels and text in figures a) and b) are small and hard to read without zooming in; colors for velocity misfit are hard to map back to the colorbar because the circles are small. Would be worth discussing if these misfits are reasonable and how that is evaluated, not just that the misfit is minimized without overfitting
We increased label and text size for a), and b) and added "Velocity misfits obtained with these parameters are of similar magnitude to previous studies (e.g. Cornford et al., 2015; Schannwell et al., 2018)." to demonstrate that our misfits are of similar magnitude to other studies.

Pg. 8, Line 10: Are you referring to the magnitude of the SMB? It isn't clear in this sentence The following point ". . .we adjust the SMB using the observed model drift following the relaxation simulation" also isn't clear to me what you have done, would be good to elaborate more and to explain better why this is reasonable to do. The following sentences are also not clear to me, especially "we treat the unadjusted SMB as a simulation with a perturbed SMB" – are there some words missing?
We reworded this section to make it clearer what is done here. It reads: "This asymmetric SMB pattern is consistent with observations (Drews et al.,2013), but does not capture the correct magnitudes. Therefore, we adjust the SMB using the computed model drift following the relaxation simulation. This means for the reference simulation, the SMB forcing consists of the RACMO2.3 field plus the computed spatial thickening/thinning rate (model drift) at the end of the relaxation simulation. This approach ensures that the model drift is eliminated and the divides stay at their initial position. Since without this model drift correction, there is a change in divide position, we treat the unadjusted SMB as a simulation with a perturbed SMB."

Table 2: Is there a misplaced mention to "Run 6", or what does SMB forcing mean here?
No, it is all correct. As is written in the text: "To permit a more direct comparison between ocean forcing and SMB forcing, an additional SMB perturbation simulation is performed, where the SMB is unadjusted and the initial grounding-line flux perturbation from the shelf removal simulation on either side of Halvfarryggen is added to the SMB term (Table 2, Run 6). This is done such that the spatial pattern of the SMB remains unchanged, but the magnitude is different by about a factor two in comparison to the unadjusted SMB."
To facilitate connecting this to the correct simulation run, we added a reference to the specific run.

Figure 4: In this case the text fonts are so big it is almost distracting to what you are trying to show (but readable!). Mesh elements should be two words.
We have decreased the font size.

Pg. 10, Line 3: I know that it is used, but "inverted basal drag coefficients" sounds funny, so maybe state that these are found by solving an inverse problem
Changed.

Do these two cases use the same regularization parameters?
Yes, as stated in the Model initialisation section: ”The Tikhonov parameter from the SSA inversion was used for the FS inversion as well.”

Is an order of magnitude difference as significant as it sounds?
Yes, it is. As stated in the text, in the simulation using the SSA basal friction coefficients, there is a thinning rate of 200 m/century and in the simulation using the FS basal friction coefficient, this trend is absent!

Pg. 10, Line 8: Would rephrase “in divide proximity” to be “in the proximity of the divide”, or even better “near the divide”
Changed.

Pg. 10, Line 9: What should the reader take away from the statement “Thinning rates were much smaller when using the FS forward model” – what lowering rate was estimated and how did you know that was “good enough”?
We added that they are <50 m/century for the FS inversion fields. For our purpose, it would not have made a big difference as we correct for this model drift, but the wider implications for realistic projections are that the mechanical forward model and the mechanical model for the inversion should be the same.

Figure 5: Panel b) title should be “FS” and not “NS”
Changed

Is there no way to have these on the same color scale? Or, use a different color range as it is just too tempting now to compare them side-by-side
Axes labels are too small to read.
Increased axes labels and plotted both Figures on the same color scale at the cost of losing some detail in each plot.

Pg. 11, Line 5: should be “exceeds”
This refers back to thickening rates, so we think that “exceed” is correct.

Pg. 11, Line 7: Would be helpful to say the duration of the simulation here (1000 years?)
Added.

Pg. 12, Line 9: By “disparity” used here do you just mean “difference”?
Yes, changed accordingly.

Is there more to say about why the flux is so different between east and west, other than that was the forcing that was setup?
No, it is just a result of the geometry of the ice rise.

Figure 6: I spent a long time trying to figure out what is plotted here, so for what that is worth it may be better to plot and/or describe this differently. - the concept of a swath profile wasn’t completely clear, or at least would be good to explain more about why the

swaths were chosen in these locations - I didn't understand what was meant in the caption by "backward migration"
We have added a paragraph to the main text which explains how divide positions were computed and highlight that the plotted values are averaged along the swath profile and why the swath profiles were chosen in the way they are. The paragraph reads: "Divide positions are computed at every timestep along two swath profiles (~8 km and ~23 km for Halvfvarryggen and Söråsen, respectively (e.g. Figure 7)). The shorter swath profile for Halvfvarryggen was chosen to permit a simple flux balance analysis. The initial start point of the divide is the location of highest surface elevation. From this point, the divide is tracked along the swath profile by following the minimum direction of the aspect gradient until the end of the swath. Computed mean divide migration amplitudes are then averages along the swath profiles (e.g. Figure 6)."
We also added an arrow pointing to the start of the "backward migration". It is the point at which the divide migration amplitude in the refined simulations starts to decrease.

- Would help to explain more about what the values of balance flux mean in relation to understanding about how different forcing imprints a different history on the ice rise - axes labels are too small
We plot balance fluxes in order to investigate whether we can see a confirmation of the model results that show the regular mesh does not exhibit this backward migration whereas all more refined mesh simulations do. The plotted balance fluxes confirm this as they are almost equal in the regular mesh simulation, and vary greatly for the refined mesh simulations. Axes labels have been made bigger.

Also, why have these four panels together, would it be better as two figures with two panels each? Or, explain more what we learn by looking at the time series of balance flux as I had a hard time connecting to the point there.
We have changed the layout to a 2x2 format to make the Figure more readable.

Figure 7 was also hard to take in all the information shown, especially with such a bright color scale I had to zoom more to see the lines and try to relate them back to the different runs and what was shown in the other figures. I appreciate this is hard to plot, but more text around what you are plotting – and why – would help.
Also, how and why were "selected times" chosen?
As requested by reviewer 2, we have dropped the 2 km simulations from Figures 7 and 9 and have combined these two Figures to one. To better explain what the Figure is showing, we have expanded the Figure caption and now elaborate on what we mean by "selected times".

Figure 10 also took awhile to work through. Some comments: - "total mean divide migration" isn't clear how this was calculated, especially vs. "mean divide migration" - axes labels are too small - the units of the GL flux perturbation aren't intuitive – is the relative difference what is important here?
Apologies. "Total mean divide migration" was a typo. In all cases we mean "mean divide migration". A brief description of how this was calculated has been added to the manuscript. To highlight the importance of the short time period of the perturbation, we added some text to subfigure c. Axes label's fontsize has been increased.

Pg. 21, Section 5.2: I'm sorry if I lost the point here, but is these ice rises have been stable for 9ka then why investigate divide migration here over 1kyr timescale? It would be helpful to connect what you are constraining about this specific site's history to all the calculations that have been done investigating generalized forcing. I guess that I thought some of these cases may have happened here, but if not that should be really clear (and sorry if I missed it)
Ideally we would have liked to investigate longer timescale than 1kyrs, but due to the high computational costs of the FS model, we are restricted to 1kyrs. The forcing is also not tailored to a specific event e.g. transition from LGM to Holocene, but only looks at the what divide migration rates result from realistic perturbations to the SMB and ocean forcing. From our simulations over 1kyrs for the SMB simulations, we draw the conclusion that if a perturbation like this had happened over the last 9000 years, the Raymond stack would still show it today. As this is not the case, we conclude that a perturbation of this magnitude has not happened over the last 9000 years.

Pg. 24, Line 10: Do you mean "cause" larger divide migration rates, or that these configurations could experience larger migration rates?
The latter. Changed accordingly.

Pg. 26, Line 10: Should be "prove useful"
Fixed.

As a general question, is this work all about understanding past behavior, or can this understanding of how physical mechanisms drive divide migration inform us about the sensitivity of ice rises and possibly some ice rises that have configurations that make them more vulnerable to ungrounding. Or, is the divide migration focused on here not significant enough to affect ice-rise stability
We believe that these mechanisms together with the finding that subglacial topography seems to be a first-order control on divide position stability, definitely means that some ice rises are more stable than others. The model setup is easily extended to other ice rises all across Antarctica and the next step will be to test these findings on other ice rises around Antarctica with different bedrock topography settings and different ice shelf settings.

**Reviewer 2**

1 Overview:
As the title states, this work attempts to understand the kinematic responses of ice- rise divides to changing oceanic and surface mass balance (SMB) forcing, with an aim to understanding the causes of past ice-rise migrations evident in observations of isochrone patterns in existing ice rises. The authors initialize their model to match present-day conditions for two East-Antarctica ice rises, and then perform a set of numerical experiments to examine the effects of surface-mass-balance (SMB) forcing and ocean forcing (via ice-shelf thinning). the experiments are well-conceived and the results show an interesting differentiation in the rates of response as seen in the ice-divide positions. This is a nice piece of work which deserves publication after some issues have been resolved.

My biggest concern is that the simulations are under-resolved. In fairness, the issue is mentioned in the text, but mostly in passing, when in reality, under-resolution has the

potential to call all of the results in this work into question. It's clear that the "regular"-mesh runs are under-resolved, given the major differences between the "regular" mesh and the "refined" 500m one. The 350m mesh looks promising, but you need another data point to demonstrate that you're in the convergent regime, since the regular→500m→350m runs don't appear to show any sort of consistent trending behavior (I'm specifically looking at the long-term behavior in figure 6a here – assuming I'm reading the results correctly, the trend from "regular"→500m is to reduce displacement, then the trend from 500m→350m is to increase displacement, so there's not much of a consistent convergence signal). Ideally, you'd run one demonstration run finer than 350 m which would reinforce the trend from 500m→350m and would demonstrate that the 500m mesh is sufficiently resolved to capture the same dynamics as the more-refined solutions. Otherwise, you really don't have a lot of confidence that you're entering the asymptotic regime. I do realize that might be computationally unattainable. A shorter test run may well be sufficient to make this case.
We absolutely agree that mesh resolution is crucial and also agree that the regular mesh is under-resolved. We also agree that yet a finer resolution would be desirable.
To address this, we performed two additional simulations.

- The first simulation performed the no-shelf simulations at 350 m resolution, and shows that convergence is present albeit not at first order. Please note that the simulation is not finished yet (at ~350 years), but Figure 8 will be updated once the simulation has finished.
- The second simulation we performed used a 250 m resolution at the divide and 2 km elsewhere. However, this simulation only confirms that high resolution in both areas is needed.

We tried to run a simulation with 250 m resolution at the divides and the grounding line. This increases the problem size from 1.3 million nodes to ~4 million nodes, and is beyond the capabilities of our current direct solver setup, as we would need >64 GB memory per node. We have identified this problem and are currently working on an iterative solver setup that will permit higher resolution runs in the future. However, at the moment this is beyond the scope of this manuscript.
Please also note that we are reporting mean values along the swath profile which may not be the best quantity to gauge sufficient mesh resolution. To highlight this, we have added local maximum migration amplitudes which are 2.3 km for Halvfarryggen and 1.3 km for Söråsen in the no-shelf simulations. This corresponds to ~4-7 gridcells for Halvfarryggen and ~2-4 gridcelss for Söråsen, depending on the chosen refined mesh resolution. Therefore, while we might be under-resolving in some areas, this is not the case for the length of the swath profile.

In all honesty, there doesn't seem to be much point in spending as much time and space as you do on the "regular" mesh results, since they are so clearly under-resolved as to be of dubious value.
We agree and have shortened the text regarding the regular mesh in the discussion section. We are now also clearly stating that this mesh resolution is insufficient, especially for the ocean perturbation simulations.

I'm also concerned about trying to glean so much information from ice divide positions when much of the response is distances which are less than a single mesh cell. Is there perhaps another quantity which might be useful to reinforce your conclusions?

This is true for the ocean perturbations and yet higher mesh resolutions would be desirable. That is why we chose to perform an additional no-shelf simulation at 350m. However, anything higher is not possible as we are restricted by the availability of our computational power. We would also like to point at that this is a mean value along a 16 km swath. This means that in some areas there is almost no divide migration and in other areas larger values that the mean (see above). We added a sentence that even higher mesh resolutions may improve our results. It reads:" The low migration amplitudes also show that the employed mesh resolution (~500 m) may be insufficient for the intermediate scenarios, but owing to computational restrictions this is the highest resolution possible."

In modeling, integrated quantities are often more useful for filtering out any mesh-dependent noise. Perhaps some sort of weighted moments of the ice thickness or patterns of changes in ice thickness would be useful here.
We still believe that divide migration amplitude is the most intuitive measure and would like to keep this unchanged.

Specific points:
1. Figure 1: You should note in the caption that the inset figure (b) is rotated with respect to the full-continent figure (a).
Done.

2. p2, line 9; "ice-dynamic archive" should be "archives"
Changed.

3. Figure 2: It would be helpful to point out that subfigure (e) doesn't necessarily correspond to subfigure (b) and subfigure (f) doesn't necessarily correspond to subfigure (c), although the layout encourages that assumption.
We added to the caption: "(e) and (f) are not necessarily the result of forcing in (b) and (c), respectively."

4. p3, lines 6-9. It would be helpful if these two sentences were re-ordered to match the ordering in figure 2 (e-f). (fast migration, then slow)
Changed.

5. p 4, line 2: "relict" -> "relic"
Changed.

6. p4, line 24: "km2" should be km2 (2 should be an exponent)
Corrected.

7. p4, line 32: "... ice shelves receive..." – should it be "ice shelves provide"?
Yes. Changed.

8. p5, line 5: (possibly too pedantic on my part), I'd suggest "a complete description" instead of "the most complete...". Also, I'd suggest changing "FS flow model" to ' "full-Stokes" (FS) flow model' for accessibility.
Changed.

9. p7, line 1: I'd suggest changing "sea pressure is prescribed" -> "hydrostatic sea pressure is prescribed"
Changed.

10. p7, line 21: you have "Jm" twice instead of "Jm" and "Jp". Likewise, line 23 has two λC's and two Jreg's
Apologies. This has been corrected.

11. p8, "Experimental design" –
(a) Can the grounding lines move/retreat in your model, or are they held fixed?
Yes, we added: "In all perturbation simulations the grounding line is permitted to freely evolve."

b) How do you handle the 1km or so of remaining ice shelf once you remove the downstream shelf in the shelf removal experiments?
As stated in the Experimental Design section: "This ensures that the same frontal boundary conditions as for the SMB perturbations still apply to this geometry." The applied frontal boundary condition is listed in the Boundary Conditions sections: "For the ice shelf front boundary, the true vertical distribution of the hydrostatic water pressure is applied and the calving front is held fixed throughout the simulations."

For example, is the shelf thickness maintained at the original thickness profile? If it is allowed to change, what constraints on shelf thickness are maintained?
As stated in the Experimental Design section, only for the intermediate scenario is the thickness of the shelf kept constant. So for the extreme shelf removal simulation, there are no constraints for shelf thickness. If the shelf was thinner than 10 m, the model would keep this 10 m of shelf thickness for numerical stability reasons. As this does not happen in our simulations, we do not mention it in the text.

(I could, for example, envision a response to downstream shelf removal in which velocities in the shelf remnant (and in the upstream grounded ice) increased, causing an increase in shelf flux, which could lead to thinning and grounding-line retreat.)
This is exactly what does happen and what we are investigating in our simulations.

Also, what forcing (subshelf melt + SMB + calving rules) do they see?
Ocean and SMB forcings are summarised in Table 2 for each of the runs. Details are provided in the Experimental design section. As for calving rules, it is stated in the Boundary Condition section that we keep the calving front constant, which means no "calving law" is applied.

12. Figure 5(b): Caption above should be "FS friction coefficient", not "NS" (unless you're actually solving the Navier-Stokes equations)
Changed.

13. Somewhere in the problem description, it would be useful to show the bedrock geometry you're using, to make it apparent that the ice rises seem to be on non- retrograde bed slopes, for example.

We have added a Figure to the discussion section, where we show two cross sections of the subglacial topography of Halvfarryggen and Söråsen, underlining the point of prograde sloping bedrock topography for both ice rises.

14. Somewhere in the text, clearly describe how ice divide positions are computed. You refer to the swath, and I think you're computing averages over the swath, but it's not clear how that's done. In particular, I'm more than a bit concerned that the changes in position that you're reporting are less that a single mesh spacing. How long is the swath? Do you see evidence that the ice divide could be rotating relative to the swath-normal direction?
The reviewer is correct that we computed averages along the swath profile (see above). We have added a brief description of how divide positions are computed to section 4.2. It reads:" Divide positions are computed at every timestep along two swath profiles (~8 km and ~23 km for Halvfvarryggen and Söråsen, respectively (e.g. Figure 7)). The initial start point of the divide is the location of highest surface elevation. From this point, the divide is tracked along the swath profile by following the minimum direction of the aspect gradient until the end of the swath. Computed mean divide migration amplitudes are then averages along the swath profiles (e.g. Figure 6)."
There is no indication of divide rotation. However, even if there was, our algorithm would still find the new divide position. Only the distance computation would become more difficult, but that is not the case in our simulations

15. Figure 6:
(a) The figures are too small to be legible on a printed page – they're only usable by zooming in on the electronic version. Please make them larger (perhaps a 2x2 layout). thicker lines would help as well. Please ensure that the printed-page version of the figure is usable.
We changed the Figure format to a 2x2 layout and also increased line thicknesses to improve readability.

b) In subfigure b, there is a jump in the displacement followed by a retreat around 350-400 years which occurs at the same *time* in the different- resolution runs (vs. at the same displacement location), which seems to indicate that it's being driven by something in the external flow. Can you comment on that? Do you have any idea what's causing it? It seems unlikely to be simple noise since it shows up in more than one experimental run.
Are you talking about the refined mesh simulations? If so, we double-checked, there is no external forcing explaining the features, but since the divide is in some areas less well defined than in others that this might be the reason for this jump.

(c) Subfigures c and d demonstrate conclusively that the "regular" mesh is under-resolved. Could you include the results from the 350m run on subfigure (d)? If they're similar enough to the refined 500m results, they would bolster the case that the 500m results are useful.
We have added the 350m simulation and it indeed shows a very similar pattern to the 500m simulation. This has been added to the discussion section.

16. Figure 7: It's not clear how useful showing "regular" mesh results is, since they're demonstrably under-resolved.
We agree and have dropped the 2 km simulations from the Figures 7 and 9 and have combined these two Figures into one.

17. Figure 8:
(a) As with figure 6, these plots are unreadble on the printed page. A 2x2 layout would probably be more useful here as well.
Changed as Figure 6.

(b) Could you do a 350m finest-resolution run for the ocean-forcing (shelf removal) case as well?
Done

18. Figure 9: As with Figure 7, it's not clear how useful showing the "regular mesh" results is.
See above.

19. Figure 10:
(a) I think you've mislabled the two 90% lines? (the trends would make more sense if the East-90% and West-90% lines were swapped). If that's not the case, then it would be useful to swap them anyway and have line-color denote forcing amount, and solid vs. dashed represent east-west.
Yes, indeed it was. Changed accordingly.

b) Could you increase the vertical size of subfigure c? It's hard to discern what's going on after 5-6 years, particularly whether the lines stay above y=0. Additional stretching of the plot in the y-direction would definitely help here.
We have stretched the subplot c to make the plot clearer.

20. p19, line 8: "appears more less distinct" – presumably it's either more or less, unless you're aiming for a second career in politics.
Yes. Corrected to "less distinct"

21. Figure 12:
(a) Any idea what's causing the Cartesian-mesh-like artifacts in the $|\nabla(\text{aspect})|$ fields? I find them puzzling since you're using an unstructured mesh and they seem to be definitely some sort of Cartesian grid artifacts.
The reviewer is correct. For this plot, we regridded the output onto a Cartesian-grid for this plot. We have added this fact to the figure caption.

(b) The jumps in subfigure f could be numerical noise on the order of the mesh spacing, couldn't they?
Yes, they could. As mentioned above for the divide, the triple junction is also not always very clearly defined. So the high-frequency oscillation should not be overinterpreted.

22. p 21, section 5.2. You do a very nice job here of discussing the resolution issue. I'd suggest again that there's not much point in discussing specifics of the "regu- lar" mesh results, other than to reinforce that the 2km mesh is under-resolved.
Agreed and done. See comments above.

23. p21, line 27: You spend some time here discussing rates of dynamic response. How do you choose the timesteps for the different runs? Is $\Delta t_{regular} > \Delta t_{refined}$? If you're reducing

the timestep for the finer-resolution runs (which is reasonable), could faster dynamic response be a product of finer temporal resolution instead of the finer spatial resolution?
No this is not the case for our simulations as we always use the same timestep of 0.5 yrs as listed in Table 1.

24. p22, line 4. I'd suggest replacing "first order convergence between the different mesh resolutions" with "numerical convergence with mesh resolution", because the issue here is a lack of any convergence at all, not just the inability to obtain first-order convergence (you can have (positive) convergence rates less than first order which are still at least converging)
We have reworded this section, but we do not agree that we have no convergence at all. For the SMB simulations, we do see better than first order convergence as to our definition of convergence. A clear definition of what we define as first-order convergence has been added to section 4.3.1.

25. p22, line 5: I think you can confidently replace "may be required" with something like "are likely required"
Reworded. We now say that we need mesh resolution of ≤500 m.

26. p22, line 23: should "same finite amount" be "same fraction" or "same percentage" or something similar? ("amount" implies a fixed value, like 100m)
Agreed. Changed to "same percentage"

27. p22, line 24: "the divide to migrate" should probably be "the divide migrating"...
Changed.

28. Table 3:
(a) What is the value in the second column? max GL flux? value at a certain time? Integrated flux over time (in which case the units are incorrect)?
Apologies. We agree this was ambiguous. We added "at year 0" to the column headings where appropriate.

(b) Column 4 is labeled "GL Flux reduction", but all of the flux values in column 2 seem to represent flux *increases*?
Again correct. We mean GL flux reduction in relation to the shelf thickness perturbation simulations. We have added this to the table caption.

(c) In the first line of the table, when I subtract 23.65-9.553, I don't get 14.01 as in the table (I get 14.097, which would be 14.10). Am I misunderstanding what's being done here or is this typo?
Apologies. This was a typo. Double checked all other values, too.

(d) Shouldn't the 4th column be relative to the reference flux? (change in flux)/(reference flux) instead of (change in flux)/(new flux)
No, as we are inferring the flux decrease due to the shelf being present, our shelf thickness perturbation flux at year 0 serves as our "reference" flux.

29. p23, line 6. As mentioned before, if you're making the statement that things are controlled by the subglacial topography, you should show the subglacial topography at some point, preferably with a specific example.
See above. Figure has been added.

30. p23, line 19: "factor two" -> "factor of two"
Fixed.

31. p24, line: 13: "similarly susceptible...than" -> "similarly susceptile... as"?
Fixed.

32. p24, line 26: "first-order convergence" -> "numerical convergence" or "convergence with mesh resolution"
Fixed.

33. p24, line 27: "that that"
Fixed.

34. p24, line 29: "While this does not affect the results of the paper..." – That's too strong of a statement to make without some proof. You could say something like "while we believe that the dynamic results in this work are still valid..."
Fixed.

35. p26, line 10: "proof" -> "prove"
Fixed.

# Kinematic response of ice-rise divides to changes in ~~oceanic~~ ocean and atmospheric forcing

Clemens Schannwell[1], Reinhard Drews[1], Todd A. Ehlers[1], Olaf Eisen[2,3], Christoph Mayer[4], and Fabien Gillet-Chaulet[5]

[1]Department of Geosciences, University of Tübingen, Tübingen, Germany
[2]Glaciology Section, Alfred Wegener Institute, Helmholtz Centre for Polar and Marine Research, Bremerhaven, Germany
[3]Department of Geosciences, University of Bremen, Bremen, Germany
[4]Bavarian Academy for Sciences and Humanities, Munich, Germany
[5]Univ. Grenoble Alpes, CNRS, IRD, Grenoble INP, IGE, Grenoble, France

**Correspondence:** Clemens Schannwell (Clemens.Schannwell@uni-tuebingen.de)

**Abstract.** The majority of Antarctic ice shelves are bounded by grounded ice rises. These ice rises exhibit local flow ~~regimes~~ fields that partially oppose the flow of the surrounding ice shelves. Formation of ~~such~~ ice rises is accompanied by a characteristic upward arching internal stratigraphy ("Raymond arches"), ~~archiving potential past divide migration and the onset of divide flow. Information~~ whose geometry can be analysed to infer information about past ice-sheet ~~conditions can therefore be retrieved~~ changes in areas where other archives such as rock outcrops are missing. ~~However, the quantitative interpretation of the stratigraphy requires modelling and radar observations. Hitherto, ice-rise modelling has been restricted to 2D and excluded the coupling between ice shelf and ice rise. This presents a major limitation for the interpretation of ice rises as ice-dynamic archive.~~ Here we present an improved modelling framework to study ice-rise evolution using a satellite-velocity calibrated, isothermal, and isotropic 3D Full-Stokes model including grounding-line dynamics at the required mesh resolution (<500 m). This overcomes limitations of previous studies where ice-rise modelling has been restricted to 2D and excluded the coupling between ice shelf and ice rise. We apply the model to ~~the~~ Ekström Ice Shelf~~catchment~~, Antarctica, containing two ice rises. Our simulations investigate the effect of surface mass balance and ocean perturbations onto ice-rise divide position and interpret possible resulting unique Raymond Arch geometries. Our results show that changes in the surface mass balance result in immediate and sustained divide migration (>2.0 m/yr) of up to 3.5 km. In contrast, instantaneous ice-shelf disintegration causes a short-lived and delayed (by 60-100 years) response of smaller magnitude (<0.75 m/yr). The model tracks migration of a triple junction and synchronous ice-divide migration in both ice rises with similar magnitude but differing rates. The model is suitable for glacial/interglacial simulations on the catchment scale, providing the next step forward to unravel the ice-dynamic history stored in ice rises all around Antarctica.

## 1 Introduction

Ice rises are parabolically-shaped surface expressions along the margin of the Antarctic ice sheet, and they form where the otherwise floating ice locally regrounds. They are characterised by their radial ice-flow centre - henceforth referred to as ice-

rise divide - that is independent of the main ice sheet and the surrounding ice shelves, resulting in divergence of the main ice flow around the obstacle. These obstacles act as a decelerating force that restricts ice flow which is commonly referred to as "ice-shelf buttressing". More than 700 ice rises (Matsuoka et al., 2015) are distributed along the Antarctic perimeter (Figure 1a), providing additional buttressing to the ice upstream. Ice rises archive their flow history in their characteristic internal stratigraphy (e.g. Conway et al., 1999; Nereson and Waddington, 2002; Drews et al., 2015), making them potentially suitable sites for ice core drilling such as for the International Partnerships in Ice Core Sciences (IPICS) 2K and 40K Array (Brook et al., 2006).

Due to very low deviatoric stresses near the bed of the divide region and the power law rheology of ice, the effective viscosity (e.g. the stiffness of ice) is significantly higher towards the ice sheet bottom under the divide than in the surrounding areas. The stiff ice impedes downward flow under the divide in comparison to the flank regions (Kingslake et al., 2016) such that ice of the same age is found at shallower depths in the ice column under the divide compared to the flank regions (Raymond, 1983). This results in the formation of upward arches in the isochronal ice stratigraphy commonly referred to as "Raymond arches".

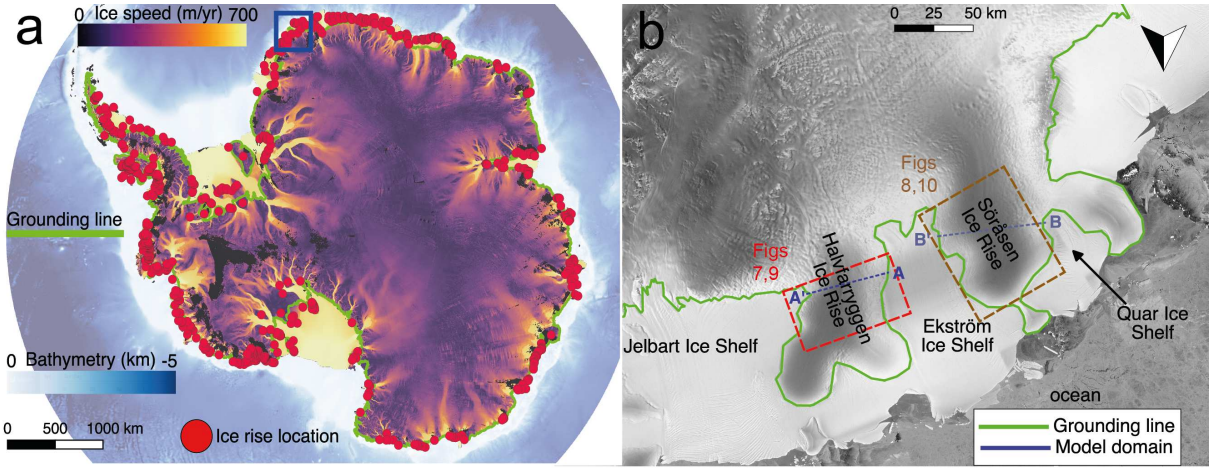


**Figure 1.** (a) Location map of ice rises along the margin of the Antarctic ice sheet (Matsuoka et al., 2015). The base map combines ice velocity of the ice sheet (Rignot et al., 2011) and the bathymetry of the adjacent ocean regions (Arndt et al., 2013). Blue rectangle shows zoom-in area of (b). (b) Radarsat image (Jezek and 5 RAMP-Product-Team:, 2002) of the study area with locations mentioned in the main text. Dashed lines (A-A', B-B') show extent of cross section shown in Figure 12. Please not that (b) is rotated by 180°with respect to (a).

Previous studies have made much progress in interpreting the Raymond arches as ice-dynamic ~~archive~~archives. The arch amplitude and the tilt of multiple Raymond arches - commonly referred to as Raymond stack - have been used to infer migration of ice divides (e.g. Nereson et al., 1998), onset of local divide flow (e.g. Conway et al., 1999; Martín et al., 2006, 2014), and ice rise residence time (e.g. Drews et al., 2013, 2015; Goel et al., 2017). Common to all these studies is the comparison of the observed isochrones derived from radar data, with the predicted age fields from models with varying input scenarios. The full stress solution of the Stokes equations is necessary because both longitudinal and bridging stress gradients are important

near ice divides (e.g. Martín et al., 2009b; Gillet-Chaulet and Hindmarsh, 2011).

~~Matching simulated arch amplitudes with observed amplitudes remains challenging and several studies (e.g. Pettit et al., 2007; Martín et al., not reproduce observed arch amplitudes with the most widely-used ice flow law (Glen's flow law, Eq. 3). It appears higher Glen flow indices than n>3 are required (Martín et al., 2006; Pettit et al., 2007; Drews et al., 2015). Observations from the Greenland ice sheet seem to support these flow conditions (Gillet-Chaulet et al., 2011; Bons et al., 2018). Moreover, an anisotropic rheology is needed to simulate double-peaked Raymond arches (Martín et al., 2009a) and ice anisotropy also impacts the arch amplitudes (Martín et al., 2014). Other challenges in modelling the internal stratigraphy include local minima in the surface mass balance (SMB) that are often not captured at the required detail in regional atmospheric models, but affect the modelled arch amplitude (Drews et al., 2015; Callens et al., 2016).~~

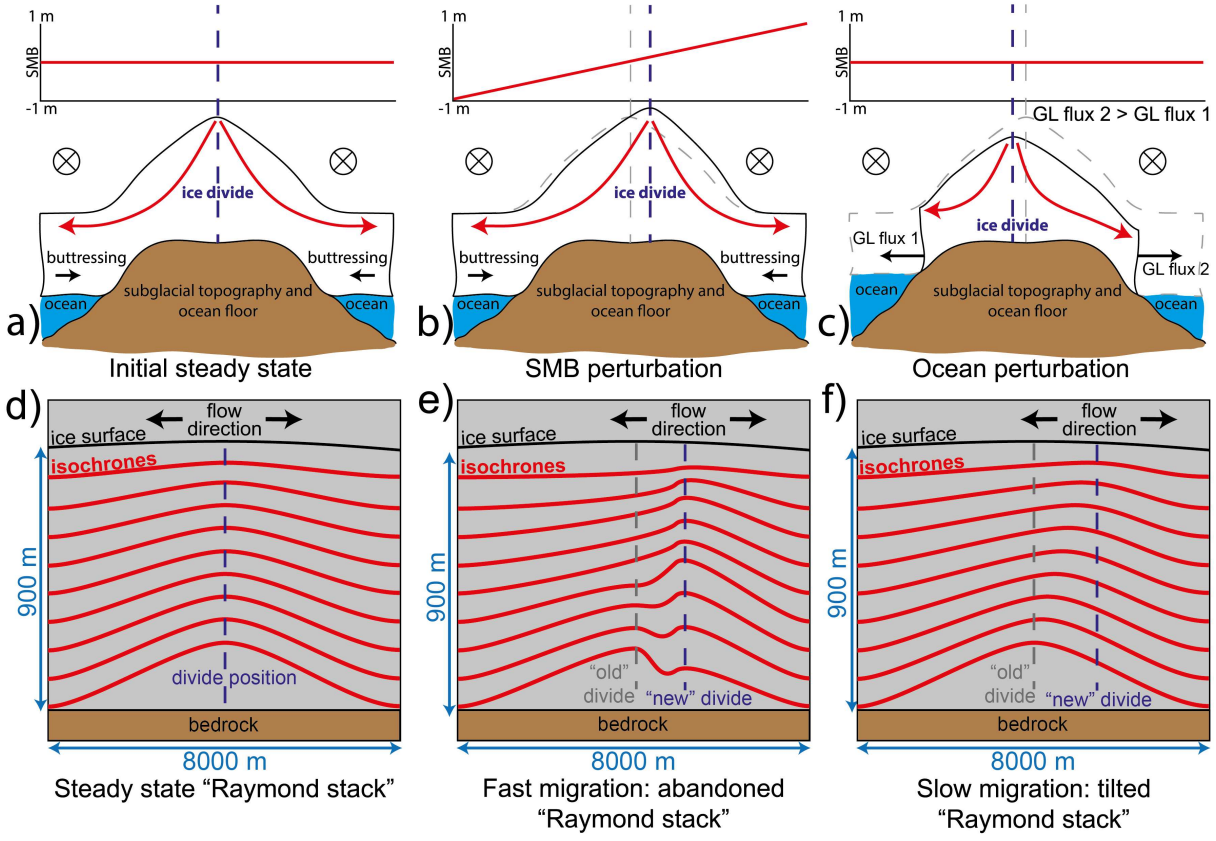


**Figure 2.** Upper panel (a-c) shows schematic steady state (a), divide migration induced by asymmetric surface mass balance forcing (b), and by ocean perturbation forcing (c). Buttressing in (c) is asymmetric. Solid red arrows indicate approximate ice flow path from ice-rise divide to ice shelf. Grey dashed lines in (b,c) display steady state geometry and divide position of (a). GL = grounding line. Lower panel (d-f) shows schematic of expected internal stratigraphy for steady state (d), fast migration (e), and slow migration (f). (e) and (f) are not necessarily the result of forcing in (b) and (c), respectively.

~~Slow migration of ice divides results in tilted Raymond stacks (Nereson et al., 1998; Nereson and Waddington, 2002; Jacobson and Wadd~~

Fast migration of ice divides results in abandoned Raymond stacks in the flanks and a new Raymond stack starts to develop at the new divide position (Jacobson and Waddington, 2005; Martín et al., 2009b, Figure 2d-f). Slow migration of ice divides results in tilted Raymond stacks (Nereson et al., 1998; Nereson and Waddington, 2002; Jacobson and Waddington, 2005; Martín et al., 200

For a new Raymond stack to form, a sudden displacement of 1-2 ice thickness is required (Martín et al., 2009b), but thus far a clear threshold between both end-member scenarios remains elusive. ~~Comparatively little is known about the stability of ice-divide triple junctions (Gillet-Chaulet and Hindmarsh, 2011). Triple junctions are points where three ice-divide ridges meet. They often coincide with the summits of ice domes. It is unclear if some transient changes in such a triple-junction setting could explain observed relict arches in ice-divide flanks, which cannot be explained with ice-divide migration in a 2D setting (Drews et al., 2015). As ice divides and triple junctions are rarely perfectly elongated or axisymmetric, three dimensional effects cannot be neglected, necessitating the use of a 3D ice-sheet model.~~ Even though divide migration has been an active focus in ice-rise research, most studies have focussed on the ramifications of divide migration (Hindmarsh, 1996; Nereson et al., 1998; Jacobson and Waddington, 2005; Conway and Rasmussen, 2009), rather than what causes the divide to migrate. ~~This is because the modelling has thus far largely~~ Additionally, modelling thus far has been restricted to 2D and ~~did not include~~ has not included interactions between ice rises and the surrounding ice shelves (Martín et al., 2009a, b; Gillet-Chaulet and Hindmarsh, 2011; Drews et al., 2015). This means that the underlying processes resulting in different Raymond arch geometries from radar observations are still incomplete and poorly constrained.

Another poorly understood parameter for ice-rise evolution are triple junctions (Gillet-Chaulet and Hindmarsh, 2011). Triple junctions are points where three ice-divide ridges meet. They often coincide with the summits of ice domes. It has been proposed that changes in triple junction position (e.g. merging of two divide ridges) might explain observed relic arches in ice-divide flanks, which cannot be explained with ice-divide migration in a 2D setting (Drews et al., 2015).

Here, we use the ~~Full-Stokes~~ full-Stokes (FS) ice-sheet model Elmer/Ice in 3D (Gagliardini et al., 2013) and extend the model domain in contrast to previous studies to include grounding-line dynamics and ice-shelf flow to study potential causes for ice-rise divide migration. We apply the model to the Ekström Ice Shelf catchment bounded by two large (15th and 16th largest in Antarctica (Matsuoka et al., 2015)) ice rises. The model is calibrated by tuning basal friction and ice viscosity so that modelled surface velocities match today's flow field. Perturbations to the SMB and ice-shelf thickness are applied in forward simulations to investigate the coupled transient response of the two ice rises. The experiments are tailored to help improve our understanding of what processes cause ice-divide migration. Specifically, we address the question of: is the amplitude of divide migration controlled by the SMB, ice-shelf buttressing, and/or is the divide position determined by the subglacial topography? Do ice rises in close proximity of each other show a similar response? Can we differentiate between the different trigger mechanisms? Furthermore, we investigate if the triple junction at one of the ice rises in the catchment - Halvfarryggen ice rise – also migrates in synchronicity with the main divide ridge

## 2 Study area: Ekström Ice Shelf catchment

Ekström Ice Shelf is located in the Atlantic sector of the East Antarctic ice sheet and is a medium-sized ice shelf. The embayment is characterised by two prominent ice rises: Söråsen ice rise in the west and Halvfarryggen ice rise, an ice promontory sandwiched between Ekström Ice Shelf and Jelbart Ice Shelf in the east (Figure 1b). While Söråsen ice rise is made up of a single ridge divide, Halvfarryggen consists of three main ridges that meet to form a triple junction close to the summit (Hofstede et al., 2013). Both ice rises belong to the larger ice rises in Antarctica with areas of about 5700 ~~km2~~ $km^2$ and 5500 ~~km2~~ $km^2$ for Halvfarryggen and Söråsen, respectively (Matsuoka et al., 2015). Söråsen rce rise is additionally buttressed in the west by Quar Ice Shelf (Figure 1b). SMB across both divide ridges is strongly asymmetric with the western downwind side of the divide receiving much less accumulation (<0.6 m/yr ice equivalent) than the eastern side (up to 2.9 m/yr ice equivalent) (Drews et al., 2013; Lenaerts et al., 2014). The catchment is a suitable test site to study the dynamics of ice rises because the boundary input datasets such as subglacial topography, ice thickness, and ice surface elevation are well constrained (with many flightlines across the region due to the vicinity of the Neumayer III airfield). In addition, the confined geometry of both ice rises suggests that ~~they receive~~ significant lateral buttressing is provided by Ekström and Jelbart ice shelves. This means that the buttressing Ektröm and Jelbart ice shelves ~~receive~~ provide also restricts ice flow across the grounding line from both ice rises, making the divide position potentially sensitive to ocean forcing.

## 3 Methods

### 3.1 Model description

#### 3.1.1 Governing equations

Ice flow is dominated by viscous forces (e.g. low Reynolds number) permitting the dropping of the inertia and acceleration terms in the momentum equations. Using these simplifications, ~~the most~~ a complete description of ice flow is the ~~FS~~ full-Stokes (FS) flow model. The Stokes equations for linear momentum are

$$\mathrm{div}\boldsymbol{\sigma} = \rho_\mathrm{i}\mathrm{div}\boldsymbol{\sigma} = -\rho_\mathrm{i}\boldsymbol{g}, \tag{1}$$

where $\boldsymbol{\sigma} = \boldsymbol{\tau} - \mathrm{p}\boldsymbol{I}$ is the Cauchy stress tensor, $\boldsymbol{\tau}$ is the deviatoric stress tensor, $\mathrm{p} = -\mathrm{tr}(\boldsymbol{\sigma})/3$ is the isotropic pressure, $\boldsymbol{I}$ the identity matrix, $\rho_\mathrm{i}$ the ice density, and $\boldsymbol{g}$ is the gravitational vector. Ice flow is assumed to be incompressible which simplifies mass conservation to

$$\mathrm{div}\boldsymbol{u} = 0, \tag{2}$$

with $\boldsymbol{u}$ being the ice velocity vector. Here we model ice as an isotropic material. Its rheology is given by Glen's flow law which relates deviatoric stress $\boldsymbol{\tau}$ with the strain rate $\dot{\boldsymbol{\epsilon}}$:

$$\boldsymbol{\tau} = 2\eta\dot{\boldsymbol{\epsilon}}, \tag{3}$$

where the effective viscosity $\eta$ can be expressed as

$$\eta = \frac{1}{2}\mathrm{EB}\dot{\epsilon_e}^{\frac{(1-\mathrm{n})}{\mathrm{n}}}. \tag{4}$$

In this equation E is the enhancement factor, B is a viscosity parameter computed through an Arrhenius law, n is Glen's flow law parameter (n=3), and the effective strain rate is defined as $\dot{\epsilon_e}^2 = \mathrm{tr}(\dot{\boldsymbol{\epsilon}}^2)/2$. Although there is evidence that the Glen flow parameter is >3 (Bons et al., 2018), particularly near ice rises (Gillet-Chaulet et al., 2011), we stick to the current modelling standard of n=3, because we focus on divide migration rather than Raymond arch amplitudes here. The same holds for the enhancement factor, which is often used to account for anisotropic effects, but is set to 1 (isotropic conditions) in all simulations. In future applications of this model, these assumptions should be revisited.

**Table 1.** Standard physical and numerical parameters used for the simulations

| Parameter | Symbol | Value | Unit |
|---|---|---|---|
| Gravity | $\boldsymbol{g}$ | 9.8 | m $s^{-2}$ |
| Ice density | $\rho_\mathrm{i}$ | 917 | kg $m^{-3}$ |
| Sea water density | $\rho_\mathrm{w}$ | 1028 | kg $m^{-3}$ |
| Glen's exponent | n | 3 | |
| Enhancement factor | E | 1 | |
| Basal friction exponent | m | 1 | |
| Basal melting tuning parameter I | G | ~~0.01~~ 0.001 | |
| Basal melting tuning parameter II | A | 0.1 | |
| Basal melting tuning parameter III | $\alpha$ | 0.4 | |
| Ice temperature | T | -10 | °C |
| Simulation length | | 1000 | yr |
| Time step size | | 0.5 | yr |
| Maximum mesh refinement | | 500 | m |

### 3.1.2 Boundary conditions

A kinematic boundary condition determines the evolution of upper and lower surfaces $\mathrm{z_j}$

$$\frac{\partial \mathrm{z_j}}{\partial \mathrm{t}} + \mathrm{u_x}\frac{\partial \mathrm{z_j}}{\partial \mathrm{x}} + \mathrm{u_y}\frac{\partial \mathrm{z_j}}{\partial \mathrm{y}} = \mathrm{u_z} + \dot{\mathrm{a}}_\mathrm{j}, \tag{5}$$

where $\dot{\mathrm{a}}_\mathrm{j}$ is the accumulation/ablation term and $\mathrm{j} = (\mathrm{b}, \mathrm{s})$, with s being the upper surface and b being the lower surface (base) of the ice sheet. The ice-shelf basal mass balance ($\dot{\mathrm{a}}_\mathrm{b}$) parameterisation follows Favier et al. (2016)

$$\dot{\mathrm{a}}_\mathrm{b} = \mathrm{H}^\alpha(\rho_\mathrm{f}\mathrm{G} + (1-\rho_\mathrm{f})\mathrm{A}), \tag{6}$$

where H is the ice thickness, G, and A ~~,~~ are tuning parameters to constrain melt rates at the grounding line and away from the grounding line, respectively, and $\alpha$ ~~are tuning parameters~~ is a local tuning parameter (Table 1). The parameter $\rho_{\mathrm{f}}(\mathrm{x},\mathrm{y})$ decreases exponentially with distance from the grounding line, varying from $\rho_{\mathrm{f}}(\mathrm{x},\mathrm{y}) = 1$ at the grounding line and $\rho_{\mathrm{f}}(\mathrm{x},\mathrm{y}) = 0$ some distance (~40 km) away from it. This ensures that highest melt rates are always specified at the grounding line and decrease exponentially with distance away from it. The tuning parameters are chosen such that basal melt rates roughly agree with melt rates derived from satellite observations and mass conservation (Neckel et al., 2012). Melt rates under the shelf are generally low, ranging from -0.2 m/yr to 1.1 m/yr near the grounding line (Neckel et al., 2012). No basal melting is applied to the grounded ice sheet.

Where the ice is in contact with the bedrock a linear Weertman-type basal sliding law is employed

$$\boldsymbol{\tau_b} = \mathrm{C}|\boldsymbol{u_b}|^{\mathrm{m}-1}\boldsymbol{u_b}, \tag{7}$$

where $\boldsymbol{\tau_b}$ is the basal traction, $\mathrm{m}$ is the basal friction component – set to 1 in all simulations, and $\mathrm{C}$ is the basal friction coefficient inferred by solving an inverse problem (see section 3.3 Model initialisation). Underneath the floating part (ice shelves) of the domain basal traction is zero ($\boldsymbol{\tau_b} = 0$), but hydrostatic sea pressure is prescribed.

For the ice shelf front boundary, the true vertical distribution of the hydrostatic water pressure is applied and the calving front is held fixed throughout the simulations. We assume the ice is isothermal with a constant temperature of -10°C. We specify depth-independent horizontal ice velocities taken from the MEaSUREs datatset (Rignot et al., 2011) at all lateral boundaries other than the ice-shelf front. To solve the presented system of equations with the appropriate boundary conditions, we use the open-source finite element code Elmer/Ice (Gagliardini et al., 2013).

### 3.2 Initial geometry and input data

To initialise the model geometry, subglacial topography was taken from the BEDMAP2 dataset (Fretwell et al., 2013). Our surface elevation is a merged product of Cryosat and, where available, higher resolution TanDEM-X digital elevation models (V. Helm, pers. communication 2018). SMB ($\dot{a}_{\mathrm{s}}$, Eq. 5) in our simulations was taken from regional climate model simulations with RACMO2.3 (Lenaerts et al., 2014). This model reproduces the commonly observed asymmetric SMB across ice rises (Callens et al., 2016). Velocity observations to match modelled ice velocities in the inversion procedure were taken from the MEaSUREs datatset (Rignot et al., 2011).

### 3.3 Model initialisation

We perform the model initialisation in two steps using two different mechanical models: the shallow shelf approximation (SSA; Morland (1987)) and the FS model. The SSA ice-sheet model is initialised by solving an optimisation problem to simultaneously infer the basal traction coefficient $\mathrm{C}$ and the viscosity parameter $\mathrm{B}$. This type of snapshot initialisation is well known and widely employed in ice-sheet modelling and aims to match modelled velocities with observed velocities (e.g. MacAyeal, 1993; Gillet-Chaulet et al., 2012; Cornford et al., 2015). In a more formal way, we seek a minimum of the objective

function

$$J = J_m + J_p, \tag{8}$$

where $J_m$ is the misfit between observed and modelled velocities and ~~$J_m$~~ $J_R$ is a Tikhonov penalty function described by

$$J_p = \lambda_C J_C^{reg} + \lambda_B J_B^{reg}, \tag{9}$$

where $\lambda_C$ and ~~$\lambda_C$~~ $\lambda_B$ are the Tikhonov parameters $J_C^{reg}$ and ~~$J_C^{reg}$~~ $J_B^{reg}$ represent the smoothness constraints of basal drag and viscosity (e.g. Gillet-Chaulet et al., 2012; Cornford et al., 2015). The smoothness constraints penalise the square of the first derivatives. An L-curve analysis was performed to ~~calibrate~~ pick the Tikhonov parameters and avoid overfitting or overregularisation (Fürst et al., 2015). The selected values are $\lambda_C = 10^7$ and $\lambda_B = 10^6$ (Figure 3). Velocity misfits obtained with these parameters are of similar magnitude to previous studies (e.g. Cornford et al., 2015; Schannwell et al., 2018).

However, when the inferred basal traction coefficient and viscosity fields from the SSA inversion were used in forward simulations, unrealistically high surface lowering rates (200 m/century) in the vicinity of the divide were observed. To circumvent this problem, the output fields from the SSA inversion were used as input for a second inversion using the FS model, but only adjusting the basal friction coefficient, while keeping the viscosity of the first inversion fixed. The Tikhonov parameter from the SSA inversion was used for the FS inversion as well. For both inversions a horizontal grid resolution of ~1 km was used. Following initialisation, as is commonly done in ice-sheet modelling, we performed a short 10-year relaxation simulation to smooth out data inconsistencies such as differences introduced by differing acquisition dates of ice surface elevation and surface velocity. This simulation length for the relaxation lies in the range of what other studies have done previously (e.g. Cornford et al., 2015; Schannwell et al., 2018).

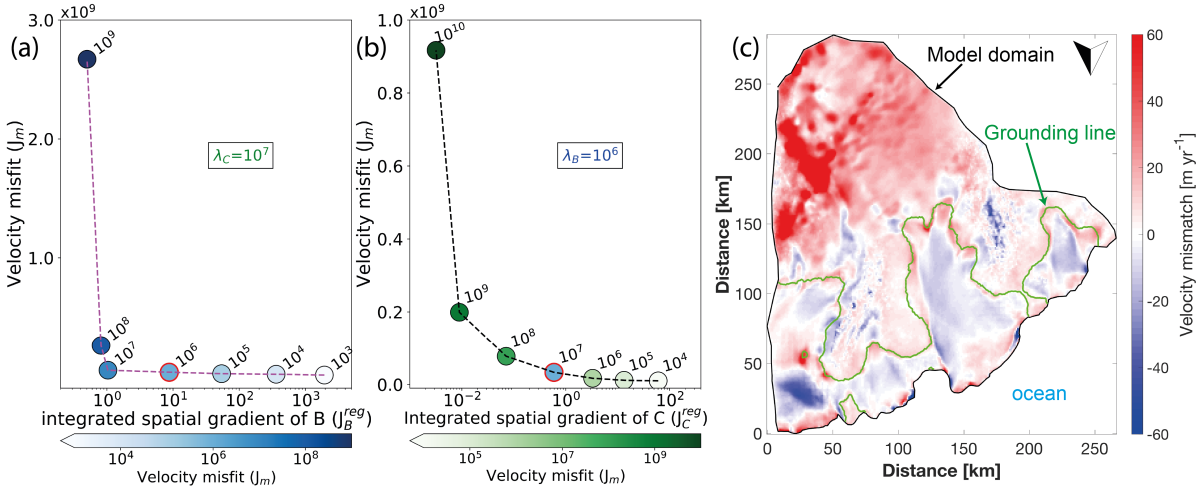


**Figure 3.** L-curve analysis to select Tikhonov parameters $\lambda_B$ and $\lambda_C$: (a) 2-D cross section for variable $\lambda_B$ and $\lambda_C$ fixed at $10^7 Pa^{-2} m^6 a^{-4}$. (b) Reverse case with constant $\lambda_B$ at $10^6 m^4 a^{-2}$ and varying $\lambda_C$. The units of $J_m$ and $J_C^{reg}$ are $m^4 a^{-2}$ and $Pa^2 m^{-2} a^2$, respectively. $J_B^{reg}$ is unitless. (c) shows mismatch between modelled and observed velocities (Rignot et al., 2011) after FS inversion for the modelling domain (Figure 1b, blue outline).

### 3.4 Experimental design

The forward simulations focus on two types of perturbation simulations (1) perturbations to the SMB, and (2) ocean perturbations resulting in changing ice-shelf thickness and hence ice-shelf buttressing. For the SMB, we use modelled values from RACMO2.3 (Lenaerts et al., 2014). The spatial pattern of the SMB is such that low accumulation rates are applied on the western (downwind) side (<0.5 m/yr) of the ice rises and high accumulation rates (>1 m/yr) are applied on the eastern (upwind) sides. This asymmetric SMB pattern is consistent with observations (Drews et al., 2013), but does not capture the correct magnitudes. Therefore, we adjust the SMB using the ~~observed~~ computed model drift following the relaxation simulation. ~~The SMB is held constant in time, and the adjustment is equal to the~~ This means for the reference simulation, the SMB forcing consists of the RACMO2.3 field plus the computed spatial thickening/thinning rate ~~and keeps all ice divides at the~~ (model drift) at the end of the relaxation simulation. This approach ensures that the model drift is eliminated and the divides stay at their initial position. ~~This is our reference simulation, and~~ Since without this model drift correction, there is a change in divide position, we treat the unadjusted SMB as a simulation with a perturbed SMB. In the second type of experiments, we perturb the reference run by thinning ice shelves through an increase in ocean induced melting. The extreme scenario, where all ice shelves are removed, is simulated by cutting the numerical mesh ∼1km downstream of the present grounding-line position. This ensures that the same frontal boundary conditions still apply to this geometry. To test more ice-shelf buttressing reduction scenarios, we performed additional model simulations with intermediate shelf thinning scenarios, where shelf thickness was reduced by 10% and 50% at the start of the perturbation simulation. For both simulations the shelf geometry is kept constant for the remainder of the simulation by applying a synthetic steady-state ocean forcing. To permit a more direct comparison between ocean forcing and SMB forcing, an additional SMB perturbation simulation is performed, where the SMB is unadjusted and the initial grounding-line flux perturbation from the shelf removal simulation on either side of Halvfarryggen is added to the SMB term (Table 2, Run 6). This is done such that the spatial pattern of the SMB remains unchanged, but the magnitude is different by about a factor two in comparison to the unadjusted SMB. In all perturbation simulations the grounding line is permitted to freely evolve. All perturbation simulations are run forward for 1000 years which is about the characteristic time T (T=ice thickness/accumulation) for Halvfarryggen and Söråsen ice rises (Drews et al., 2013). After one characteristic time, the formation of synclines in the internal stratigraphy can usually be observed (Martín et al., 2014). Most of the simulations are performed with two different mesh resolutions (Figure 4). The first isotropic mesh uses a horizontal resolution of ∼2 km throughout the domain (henceforth regular mesh), whereas for the second mesh (henceforth refined mesh), we initially use the same footprint as for the regular mesh, but use the meshing software MMG (http://www.mmgtools.org/), to refine the mesh along the grounding line and all ice divide ridges to a resolution of ∼500 m. Mesh resolution then decreases with distance away from the regions of interest to the lowest resolution of ∼10 km (Figure 4). A second refined mesh, where we refine down to ∼350 m at the divides and grounding line, was used for ~~one simulation~~two simulations. All meshes are held fixed over time and no dynamic remeshing is performed. A summary of all perturbation experiments is provided in Table 2.

**Table 2.** List of all perturbation experiments including forcings and mesh resolution

| Run # | Ocean forcing | SMB forcing | Mesh (max. resolution) |
|---|---|---|---|
| 1 | Function of distance to GL (Eq. 6) | Adjusted | Regular mesh (2 km) |
| 2 | Function of distance to GL (Eq. 6) | Adjusted | Refined mesh (0.5 km) |
| 3 | Function of distance to GL (Eq. 6) | Unadjusted | Regular mesh (2 km) |
| 4 | Function of distance to GL (Eq. 6) | Unadjusted | Refined mesh (0.5 km) |
| 5 | Function of distance to GL (Eq. 6) | Unadjusted | Refined mesh (0.35 km) |
| 6 | Function of distance to GL (Eq. 6) | Unadjusted + flux perturbation Run 6 | Refined mesh (0.5 km) |
| 7 | No shelf + function of distance to GL (Eq. 6) | Adjusted | Regular mesh (2 km) |
| 8 | No shelf + function of distance to GL (Eq. 6) | Adjusted | Refined mesh (0.5 km) |
| 9 | No shelf + function of distance to GL (Eq. 6) | Adjusted | Refined mesh (0.35 km) |
| 10 | 90% shelf thickness + adjusted ocean forcing | Adjusted | Refined mesh (0.5 km) |
| ~~10~~ 11 | 50% shelf thickness + adjusted ocean forcing | Adjusted | Refined mesh (0.5 km) |

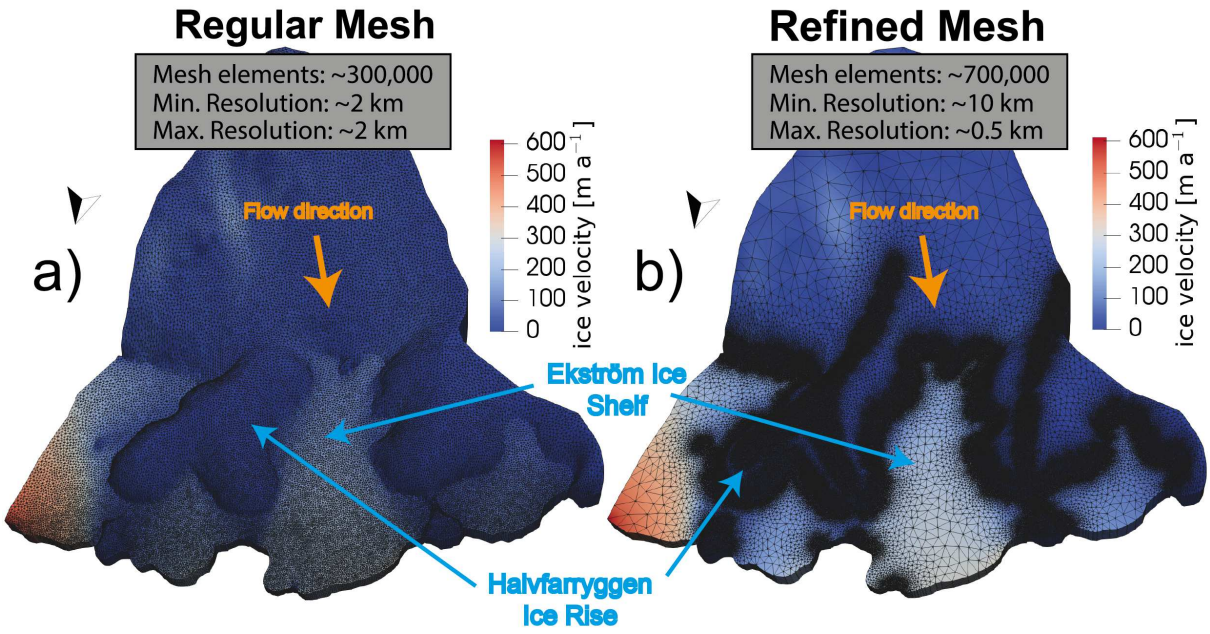


**Figure 4.** 3D plot of the model domain showing the two main mesh resolutions employed in this study. (a) shows uniform mesh of 2 km resolution and (b) shows refined mesh in areas of interest such as the grounding line and the ice rise divides. In these areas mesh resolution is ∼500 m and away from these regions mesh resolution increases to 10 km.

## 4 Results

### 4.1 Effect of mechanical model in initialisation on transient simulations

We observed an order of magnitude difference in the ~~inverted~~ basal drag coefficients found by solving an inverse problem, depending on whether we use the SSA or the FS approximation as forward model (Figure 5). This means that sliding is more restricted in the FS case in comparison to SSA case. Most notably, in comparison to the SSA inversion, the slippery regions in the FS inversion do not extend as far upstream. For example, between the ice divide of Halvfarryggen and the grounding line on either side, there are areas of stickier bedrock conditions that are missing in the drag field of the SSA inversion (Figure 5). Spuriously high ice surface lowering rates (200 m/century) ~~in divide proximity~~ near the divide were simulated when basal drag and viscosity fields were used from the inversion using the SSA. Thinning rates were much smaller (≤50 m/century) when using the FS forward model.

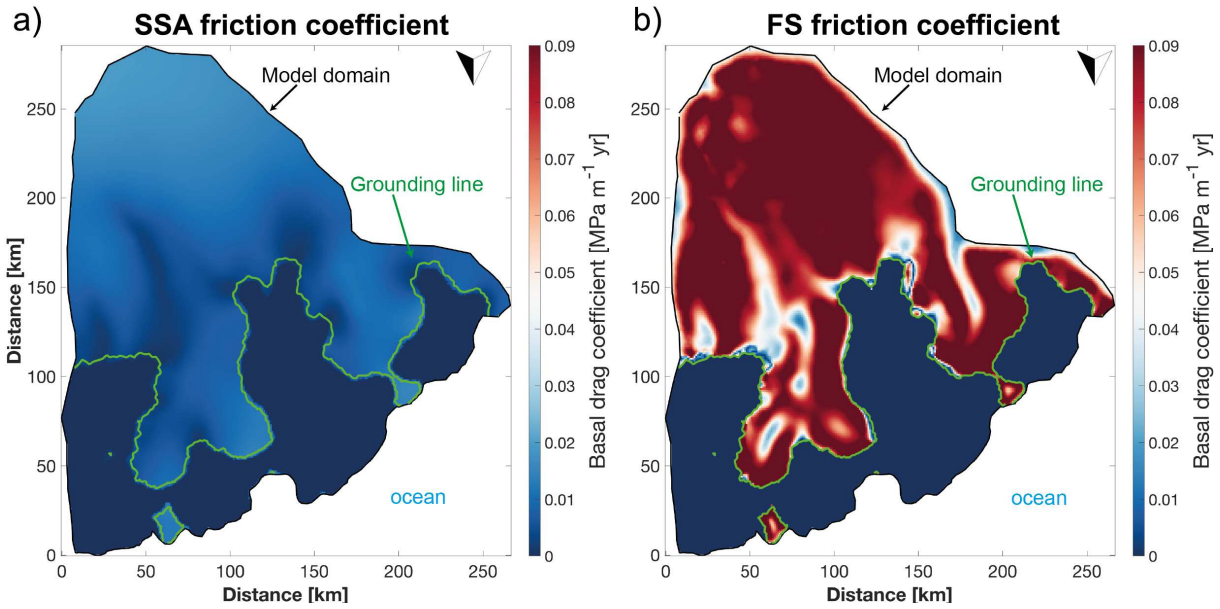


**Figure 5.** Inferred basal traction fields C using the SSA model (a) and the FS model (b).~~Note the difference in the colourbar scale.~~

### 4.2 Reference simulation (Runs 1-2)

The reference simulation serves the purpose of ensuring that the applied synthetic SMB does indeed result in a steady-state geometry in which divide positions do not migrate and surface topography changes are minimal. It then also functions as a baseline against which the perturbation simulations can be compared. The thinning/thickening rates in this type of simulation for both meshes are highest at the start of the simulation, but never exceed 0.05 m/yr near the divide region. These low thinning/thickening rates result in a steady state geometry of the model domain that is also characterised by stable positions of the ice rise divides. For both ice rises total divide migration amplitudes are <60 m throughout the forward simulation ~~.~~ of 1000

years. Divide positions are computed at every timestep along two swath profiles (∼8 km and ∼23 km for Halvfvarryggen and Söråsen, respectively (e.g. Figure 7)). The shorter swath profile for Halvfvarryggen was chosen to permit a simple flux balance analysis. The initial start point of the divide is the location of highest surface elevation. From this point, the divide is tracked along the swath profile by following the minimum direction of the aspect gradient until the end of the swath. Computed mean divide migration amplitudes are then averages along the swath profiles (e.g. Figure 6).

### 4.3 Surface mass balance induced divide migration (Runs 3-6)

#### 4.3.1 Halvfarryggen ice rise

In simulations ~~2-4~~ 3-5 (Table 2), the SMB perturbation results in immediate divide migration for both meshes (Figure 6a). For Halvfarryggen, we focus our analysis on the main (eastern) divide ridge (Figure 1b). Owing to the more positive SMB on the eastern side of both divides, the divide migrates towards this region (Figure7a~~,b~~). Almost all of the divide migration occurs over the first 200 years of the simulation before a new steady-state position is reached (Figure 6a). During the first 200 years, the entire divide migrates at an average rate of 16-20 m/yr to the east for Halvfvarryggen ice rise. This range shows there is a clear mesh dependence on the magnitude of divide migration over this timeframe (3.2-3.8 km, Figure 6a), whereas this difference is less pronounced in the steady-state divide positions at the end of the simulation (2.5-2.8 km). For the two refined meshes (Runs 4,5; Table 2), mesh dependence is still present, even if reduced, and first order convergence between the simulations is absent. This indicates that very fine mesh resolution is required to capture divide migration, but in the light of the high computational costs to run all simulations at such a resolution, we restrict ourselves to a maximum resolution of 500 m. While the averaged absolute magnitude along the swath profile is offset by about 300 m between the refined grid simulations (Runs 3,4; Table 2), the temporal pattern of divide migration is identical (Figure 6a). This is in contrast to the regular mesh, where divide migration reaches its maximum (most eastern position) after ∼200 years and remains almost stable for the remaining simulation period. In comparison, the refined mesh simulations reach their maximum divide migration at a similar time (∼200 years), but start to slowly migrate back towards its initial position until a steady state is reached after 700 years (Figure 6a). The SMB grounding-line flux perturbation simulation (Run 6, Table 2) has almost an identical steady state as the unadjusted SMB simulation (Figure 6a), despite the SMB flux ~~disparity~~ difference between east and west of the divide being twice as high. While this does not affect the steady-state divide position, it does result in faster migration with a larger maximum amplitude of divide migration (∼3.9 km vs. ∼3.4 km).

#### 4.3.2 Söråsen ice rise

Söråsen ice rise shows a very similar response – both in absolute magnitude of divide migration as well as temporal evolution of divide migration - to the applied SMB perturbation (Figure 6b) The most pronounced differences of ∼4 m/yr are in the divide migration rates (11-15 m/yr) in the first 200 years of the simulation, when most of the divide migration takes place. The mesh dependence on divide-migration amplitudes is also present for Söråsen, even though it is slightly reduced in comparison to Halvfarryggen (2.9-3.3 km, Figure 6b). Unlike Halvfarryggen, simulations with the refined mesh do not show any backward

migration of the Söråsen divide (Figure 7c~~,d~~), but reach a new steady-state position after ~300-400 years with little migration beyond this point in all simulations (Figure 6b).

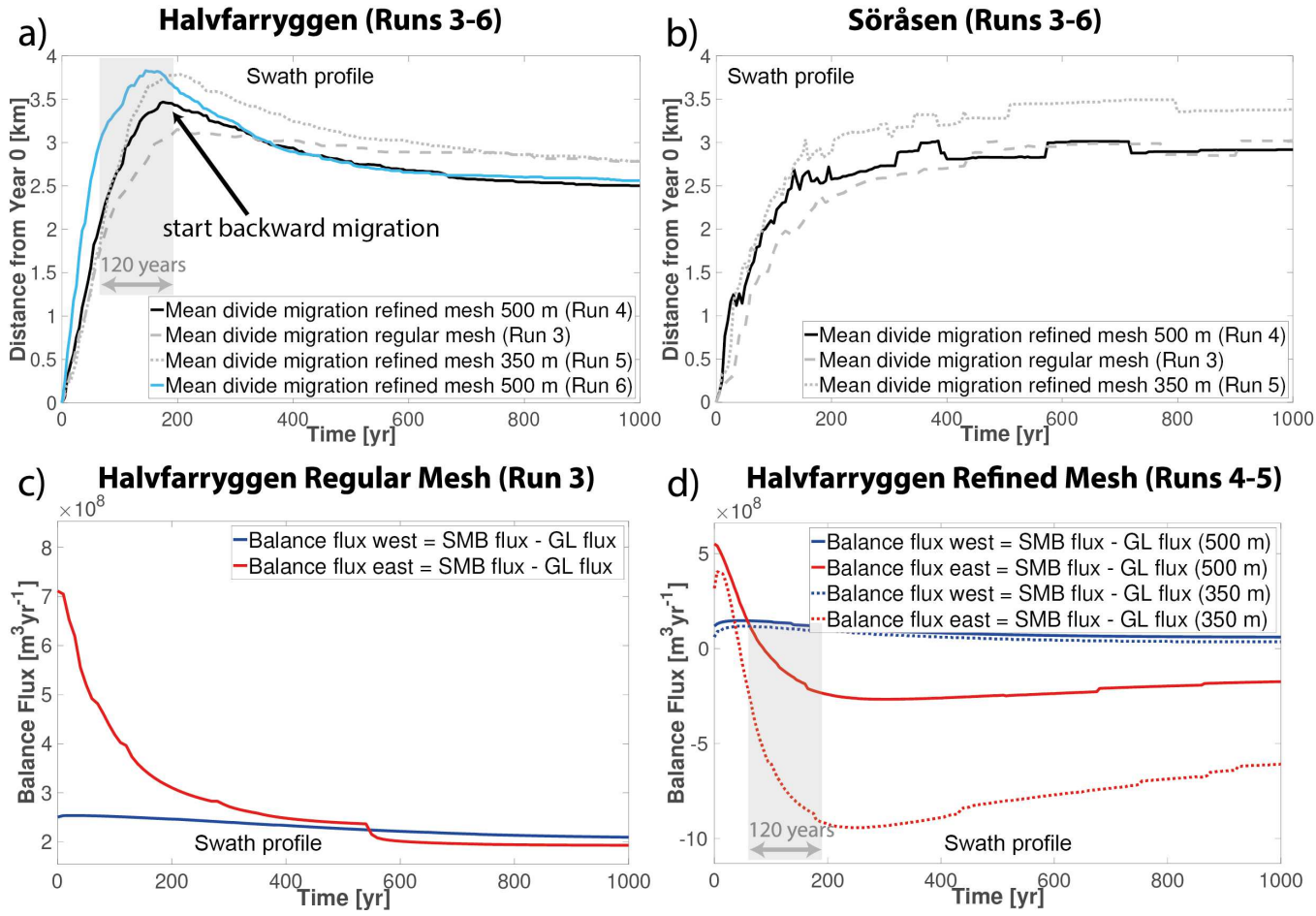


**Figure 6.** Ice-rise divide migration for Halvfarryggen ice rise (a) and Söräsen ice rise (b) induced by surface mass balance perturbation for different mesh resolutions. Positive numbers indicate migration to the east. (c,d) show balance fluxes for the eastern and western side of the divide to the grounding line for Halvfarryggen ice rise. Grey shaded areas in (a) and (d) highlight time lag between balance flux east being smaller than corresponding flux west and the start of backward migration. "Swath profile" indicates that computed divide migration is averaged over cross-sections shown in Figure 7. For the grounding line (GL) flux, this means that the flux is summed along the current grounding-line position over the swath length. The surface mass balance (SMB) flux is area averaged from the current divide position to the respective grounding-line position in the east and west of the divide over the swath length. Note different y-axis scales in (c) and (d).

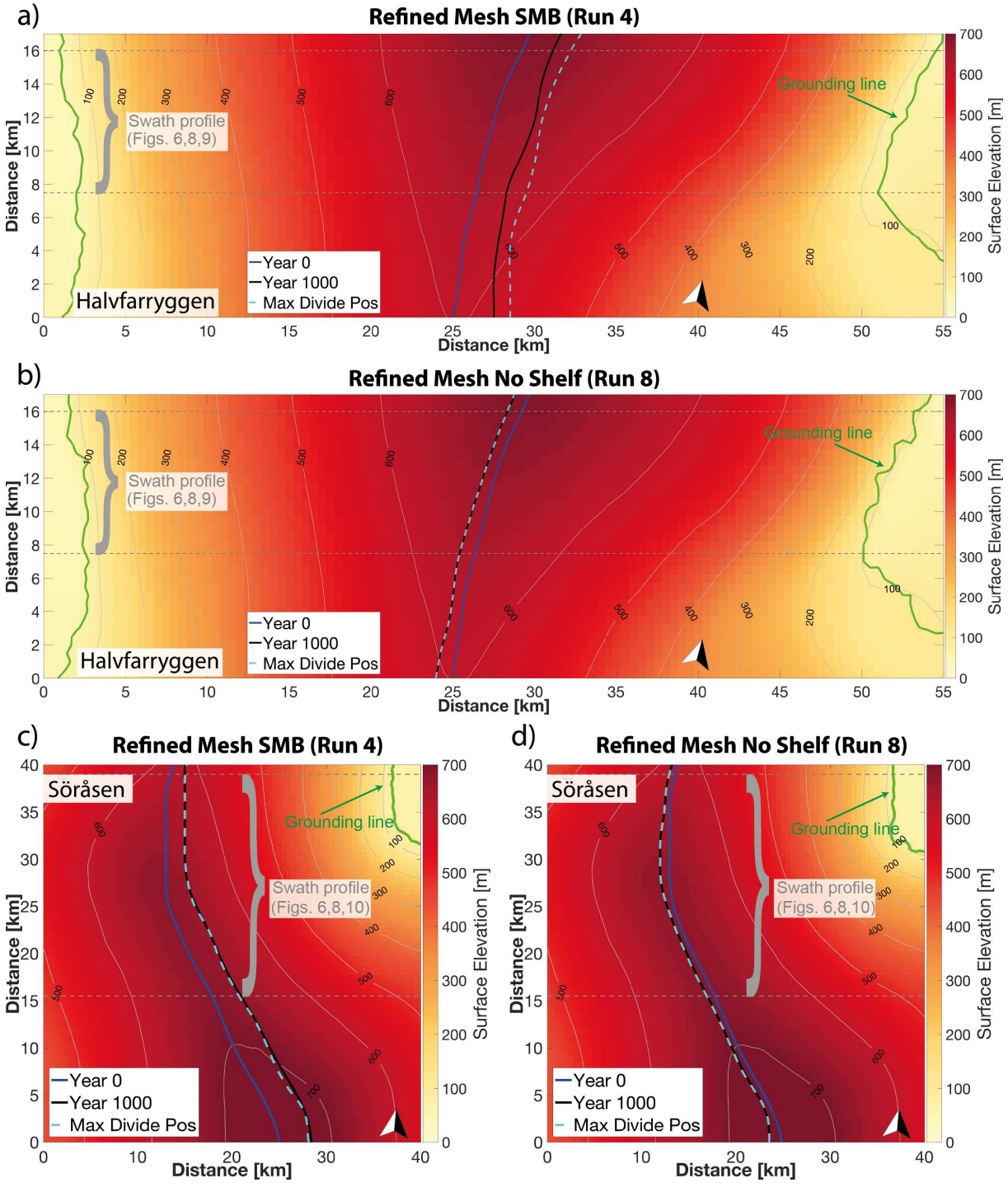


**Figure 7.** Ice-rise divide positions ~~at selected times~~ using the refined mesh for Halvfarryggen ice rise ~~(a,b) and Söråsen ice rise (c,d)~~ induced by surface mass balance perturbation ~~for the regular mesh~~ (a~~,c~~) and ~~the refined mesh~~ shelf removal perturbation (b). (c,d) show the same simulations for Söråsen ice rise. Divide positions are plotted at the start of the simulation, at the end of the simulation, and at the time of maximum divide migration amplitude for each simulation.

### 4.4 Ocean perturbation induced divide migration (Runs ~~7-10~~7-11)

Ocean perturbation causes the adjacent ice shelves to thin and reduce their ability to buttress the ice upstream. If buttressing of ice shelves on either side of the ice rise is asymmetric, this should lead to an asymmetric increase in grounding-line flux, which in turn should result in an asymmetric thinning perturbation. This asymmetric thinning perturbation should then "push" the divide in the direction of the smaller thinning perturbation (Figure 2c). In our model simulations, we test this hypothesis using the real-world example of the Ekström Ice Shelf embayment.

#### 4.4.1 Halvfarryggen ice rise

All ocean perturbation experiments result in an instantaneous divide migration. For the extreme case of ice-shelf removal (Runs ~~7-8~~7-9, Table 2) the maximum mean ice-divide migration along the swath is -0.4 km and -0.7 km ~~and occurs~~ with local maximum rates of -1.7 km and -2.3 km, occurring after 700 years and 1000 years for the regular and refined mesh, respectively (Figure 8a). Negative numbers indicate westward migration (Figure ~~??a,b~~7b,d). For the intermediate thinning scenarios (Runs ~~9-10~~10-11, Table 2), there is no divide migration for the 10% thinning scenario and -0.2 km divide migration for the 50% thinning scenario. So even though half of the shelf's thickness is removed, the magnitude of the divide migration is reduced by 77%, indicating that the response to ice-shelf thinning is non-linear and requires a strong perturbation for a significant response. Most of the divide migration takes place in the centuries following the perturbation. A stable divide position is reached after $\sim$690 years for the regular mesh simulation and after $\sim$480 years for the refined mesh simulation in the shelf removal scenario (Figure 8a). In the 50% shelf thinning scenario, a stable divide position is reached after $\sim$600 years. As was the case for the SMB, the shelf removal simulations exhibit mesh dependence with ~~the refined mesh increasing divide migration by 69%~~ mesh convergence present for the two refined meshes (Figure 8a).

To shed light on why divide migration amplitudes differ for the different shelf thinning scenario, grounding-line fluxes for the eastern and western side were computed for Halvfarryggen (Figure 8c,d and Figure 9c). In all simulations, an initial sharp increase in grounding-line flux is computed, which then quickly decays and is even lower for the eastern side of the divide than in the reference simulation (Figure 8c,d). The initial flux perturbation is largest for the shelf removal scenario and is non-linear, where halving of the ice-shelf thickness results in a flux reduction of 60%.

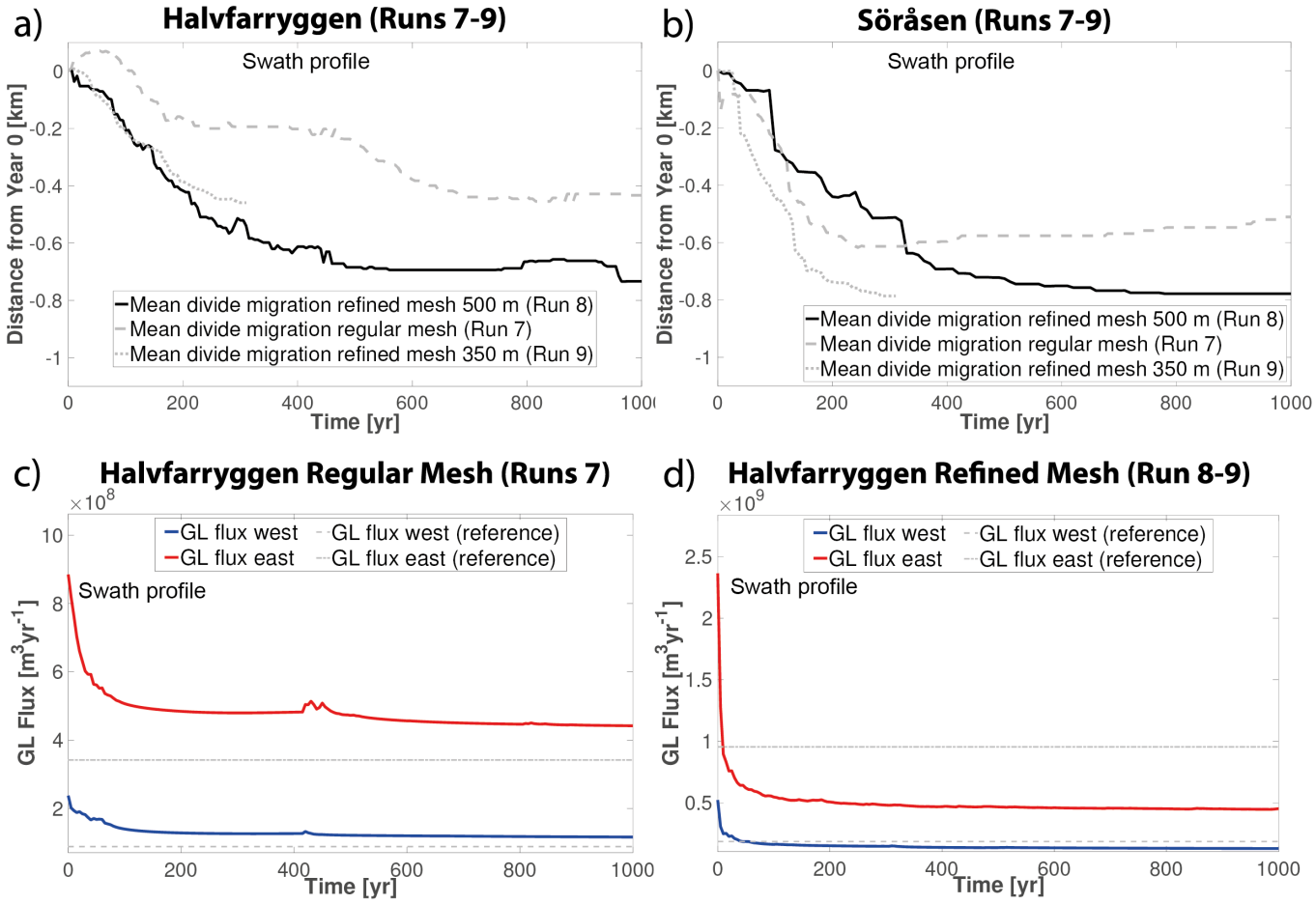


**Figure 8.** Ice-rise divide migration for Halvfarryggen ice rise (a) and Söräsen ice rise (b) induced by ocean perturbation (shelf removal) for different mesh resolutions. Negative numbers indicate migration to the west. (c,d) show grounding-line (GL) fluxes for the eastern and western side of the divide to the grounding line for Halvfarryggen ice rise. "Swath profile" indicates that computed divide migration is averaged over cross-sections shown in Figure ??7. For the GL flux, this means that the flux is summed along the current grounding-line position over the swath length. Note different y-axis scales in (c) and (d).

~~Ice-rise divide positions at selected times for Halvfarryggen ice rise (a,b) and Söräsen ice rise (c,d) induced by ocean perturbation (shelf removal) for the regular mesh (a,c) and the refined mesh (b,d).~~

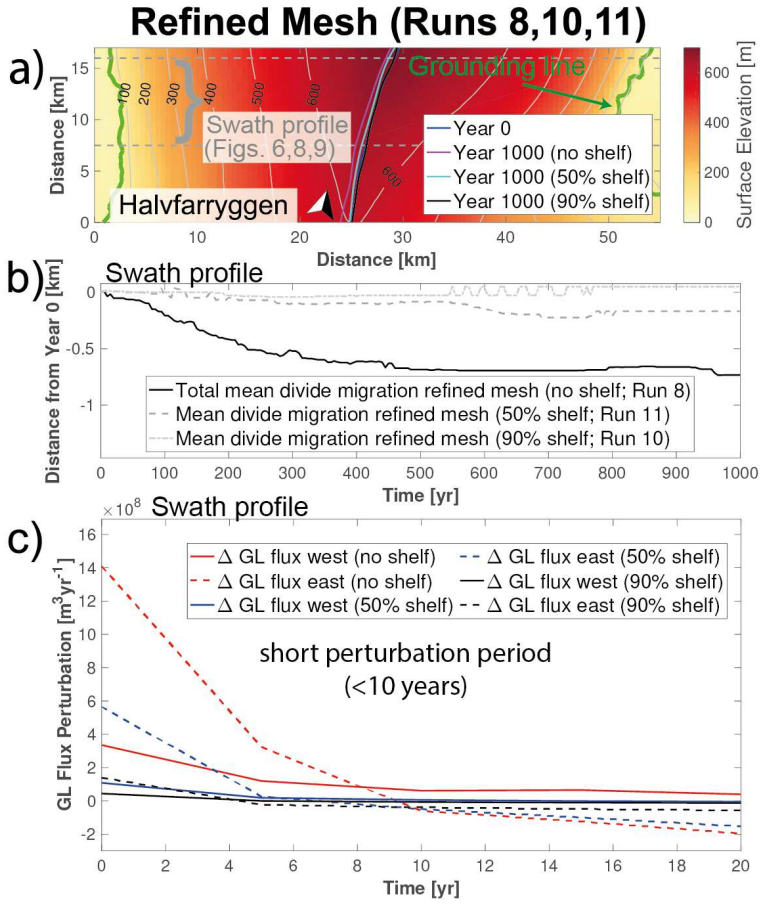


**Figure 9.** Ice-rise divide migration for Halvfarryggen ice rise induced by different ocean perturbations (shelf removal, 50% ice-shelf thickness, and 90% ice-shelf thickness) for the refined mesh (a-c). (a) shows divide position at the end of the simulation period. Grey dashed lines approximate area used for flux calculations in (c). (b) shows mean divide migration for the different perturbations. Negative numbers indicate migration to the west. (c) displays ice flux perturbation across the grounding line for the eastern and western side of the divide for the first two decades. Perturbation fluxes smaller than 0 indicate that ice flux across the grounding line is reduced in comparison to the reference simulation. (b,c) "Swath profile" indicates that computed divide migration is averaged over cross-sections as shown in (a). For the ΔGL flux, this means that the flux is summed along the current grounding-line position over the swath length.

### 4.4.2 Söråsen ice rise

For the extreme case of ice-shelf removal (Runs ~~7-8~~7-9,Table 2) the maximum ice-divide migration is -0.5 km and -0.7 km with local maximum rates of -1.0 km and -1.5 km for the regular and refined mesh, respectively (Figure 8b). Almost all of the divide migration happens in the first half of the simulation period before a new steady-state position is reached after 300 years

for the regular mesh and after ~400 years for the refined mesh (Figure 8b). This behaviour closely follows Halvfarryggen both in terms of migration amplitudes and direction (~~Figures~~Figure 8b~~, ??c,d~~). This is not the case for the intermediate thinning scenarios (Runs ~~9-10~~10-11, Table 2), where no divide migration (<60 m) occurs in any of them.

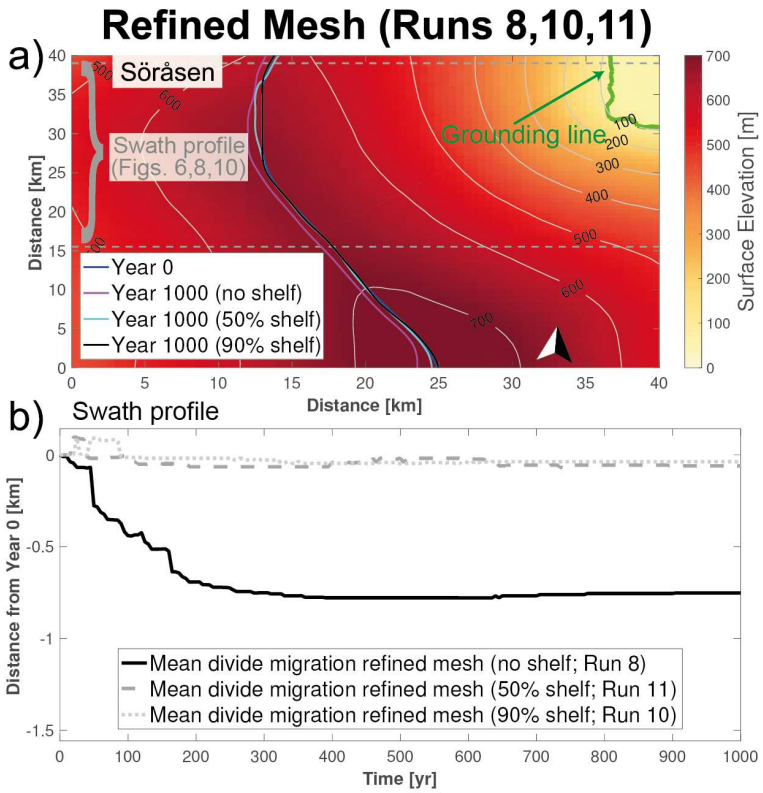


**Figure 10.** Ice-rise divide migration for Söråsen ice rise induced by different ocean perturbations (shelf removal, 50% ice-shelf thickness, and 90% ice-shelf thickness) for the refined mesh (a,b). (a) shows divide positions at the end of the simulation period. (b) shows mean divide migration for the different perturbations. Negative numbers indicate migration to the west.

### 4.5 Triple junction migration Halvfarryggen ice rise

In both experiments (Runs 4,8), the triple junction immediately migrates in response to the perturbations. The triple junction evolution closely follows the temporal evolution of the main divide. The maximum migration amplitude is 3.3 km and -1.2 km for the SMB and shelf removal simulations, respectively. Most of the triple junction migration takes place over the first ~400 years, before a new steady-state position is reached (Figure 11). The temporal evolution of the triple junction migration also shows a tendency to migrate back to its initial position in the latter part of the SMB simulation (Figure 11c). Because the SMB is most positive to the east of the main divide arm, the eastward migration of the divide leads to an increased angle between these two ridges of 3.5°, translating into a widening of 5%. In addition to the widening, the minor ridge appears ~~more~~ less distinct at the end of the simulation period (Figure 11b). This feature is absent in the shelf removal simulation. In contrast to

the SMB simulation, the westward migration of the divide leads to a narrowing of the angle between the two ridges, albeit only by 1.1°, corresponding to a narrowing of 1.4%. The main component of the migration is east-west, but in both simulations the triple junction also migrates south.

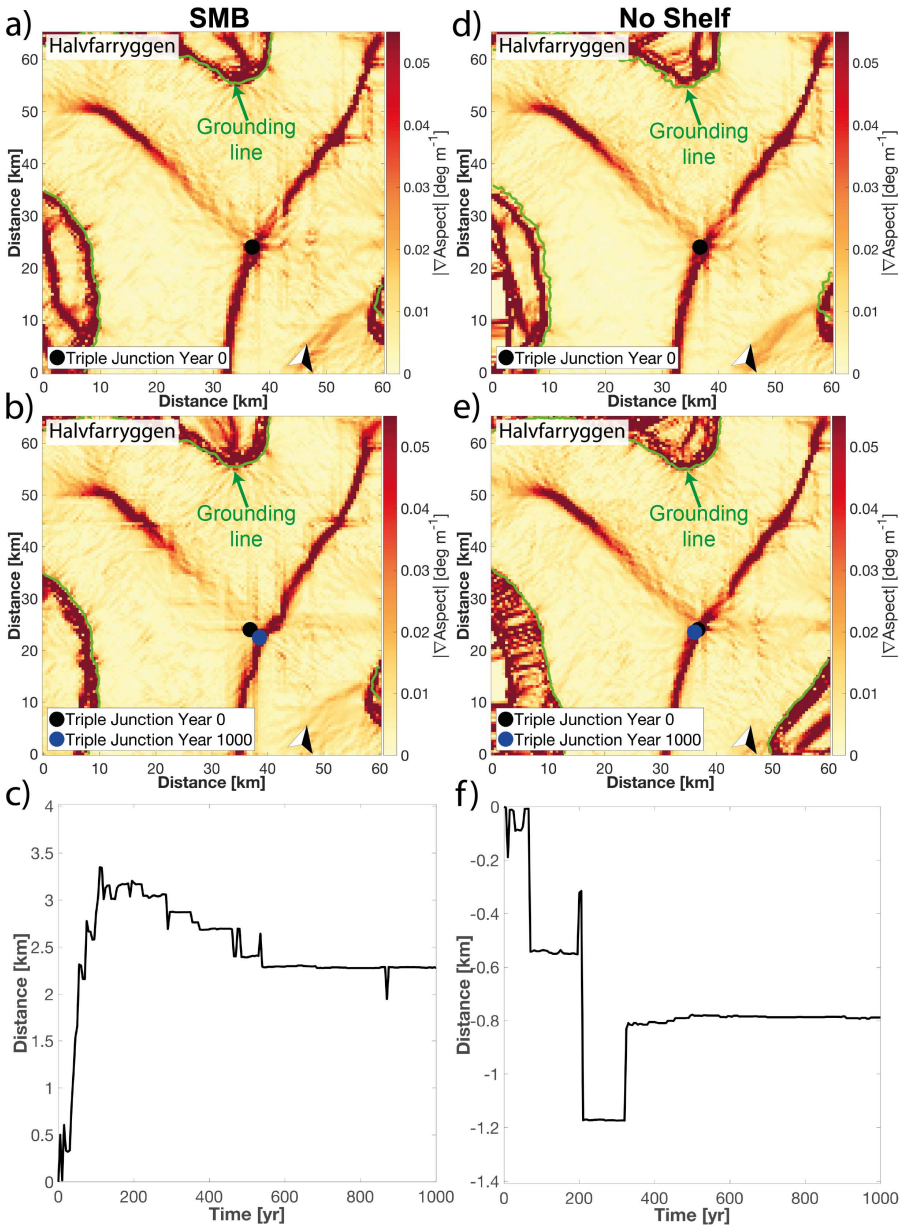


**Figure 11.** Triple junction migration for Halvfarryggen ice rise induced by surface mass balance perturbation for the refined mesh (a-c) and ocean perturbation (shelf removal) for the refined mesh (d-f). Upper and middle panels (a,b,d,e) were regridded onto a 500 m Cartesian mesh and show triple junction position at the start and end of the simulation period, respectively. Lower panel (c,f) shows mean divide migration for the respective perturbation simulations. Negative numbers indicate migration to the west. Note different y-axis scales in (c) and (f).

## 5 Discussion

### 5.1 Effect of mechanical model in initialisation on transient simulations

Transient simulations using basal drag coefficient and ice viscosity fields from the SSA inversion result in unrealistically large ice mass loss rates in the decades following model initialisation. Knowing that the Ekström catchment is likely close to a steady-state (Drews et al., 2013), we attribute these differences in the transient simulations to the difference in force balance approximation used in the inversion and transient simulation. This shows that for the presented ice-rise modelling a FS inversion is necessary for plausible transient simulations.

### 5.2 Surface mass balance induced divide migration

The computed mean divide-migration rates of 2.5-3.5 m/yr for both ice rises are higher than what has previously been inferred from the geometric analysis of Raymond stacks (0.5 m/yr Siple Dome; Nereson et al. (1998)). This means a realistic SMB perturbation, which could have occurred at the Last Glacial Macximum (LGM), leads to fast divide migration. Even more so because these migration rates are even higher (11-20 m/yr), if only the first 200 years are considered. Such a perturbation would likely lead to an abandoning of the Raymond stack and the formation of a new Raymond stack at the new steady-state divide position (Figure 2e), as the divide migrates >3 ice thicknesses away from its initial position. Because the Raymond stack at Halvfarryggen and Söråsen are well developed and it takes ∼10T (T = characteristic time, T=900 years (Drews et al., 2013)) to form such a stack, we conclude that both ice rises have not experienced a perturbation of such magnitude over the last ∼9000 years, indicating stable ice-flow conditions in this embayment for at least the Holocene time period.

For both ice rises, divide migration shows a clear dependence on mesh resolution. ~~Not only are migration amplitudes different, but for Halvfarryggen a finer mesh resolution also results in differences in temporal divide migration pattern, with~~ As the regular mesh simulations are most likely under-resolved, we will mainly focus here on the refined mesh simulations~~showing a subtle backward migration trend in~~ . In the latter half of the simulation period (Figure 6a), the refined mesh simulations show a subtle backward migration trend. We attribute this backward migration pattern to be a direct result of an imbalance in balance fluxes for the eastern and western side of the divide ~~. In the regular mesh simulation (Run 3, Table 2),the~~ (Figure 6c,d). The more positive SMB on the eastern side of the divide results in an initial increase in balance flux, which ~~slowly~~ quickly decays over time because the grounding-line flux compensates for the increased ice thickness by discharging more ice into the shelf. After ∼~~400~~ 80 years the balance flux on the eastern side is lower than the corresponding flux on the western side~~, but the difference is small and does not result in any changes in divide position (Figure 6c). For the refined mesh simulations (Run 4, Table 2), the same initial increase in balance flux is computed. But the decay occurs much quicker than in the regular mesh simulation, showing that the grounding-line flux compensates much quicker for the increased ice thickness (Figure 6d). This leads to the eastern balance flux being lower than the corresponding western balance flux after ∼80 years.~~ . However, the balance flux continues to decrease because of the continuing increase in grounding-line flux up to ∼250 years, before it recovers slightly. The negative balance flux in the east leads to the computed subtle back migration trend from ∼185 years to ∼700 years. However, the timing of when the balance flux in the east starts to be lower than the balance flux in the west is

120 years prior to this (Figure 6a,d). This means that there is a time lag of 120 years before the divide reacts to changes in the balance fluxes. The time lag may be a little smaller since the balance flux in the east is also lower than the balance flux in the west for the regular mesh simulation, but does not result in backward migration of the divide. This indicates that there must be a certain magnitude in the imbalance of the balance fluxes on either side of the divide before the divide responds to this. ~~It~~ The difference in the balance flux analysis between the regular and refined mesh (Figure 6c,d) also highlights the importance for fine mesh resolution to resolve these processes~~. In our simulations, first order convergence between the different mesh resolution (down to ~300 m) was absent, indicating that even higher mesh resolutions may be requiredto achieve this asymptotic behaviour~~, corroborating that mesh resolutions of $\leq$500 m are required. A flux analysis could not be performed for Söråsen because the selected model domain does not completely cover the ice rise.

### 5.3 Ocean perturbation induced divide migration

Since divide migration amplitude is $\leq$1 ice thickness away from the initial divide position and the mean migration rates are <0.75 m/yr, we interpret this as shelf thickness perturbations resulting in slow divide migration. Especially in the context of complete shelf removal being a rather extreme perturbation, the intermediate thinning scenarios might provide a more realistic experiment for the recent past of the Ekström catchment. The simulated small migration amplitudes for the intermediate shelf thinning scenarios (<300 m) indicate that due to the wedged-in geometrical setting of Ekström Ice Shelf, a large portion of the shelf thickness needs to be removed before any flux increase across the grounding line becomes apparent and leads to migration of the divide. This means that shelf thickness perturbations in our experiment would most likely result in a left tilted Raymond stack, rather than leading to an abandoning of the initial Raymond stack (Figure 2f). The low migration amplitudes also show that the employed mesh resolution (~500 m) may be insufficient for the intermediate scenarios, but owing to computational restrictions this is the highest resolution possible.

As all mean migration amplitudes are <1 km, we will restrict our discussion to the refined mesh simulations (Runs 8-9, Table 2). Based on our asymmetric buttressing hypothesis, a simple interpretation of our results would be that Jelbart Ice Shelf for Halvfarryggen and Ekström Ice Shelf for Söråsen provide more buttressing than their respective counterparts in the west, as the divides of both ice rises migrate to the east. However, when using Schoof's flux formula (Schoof, 2007) together with the computed initial fluxes to estimate buttressing ($\Theta$) for Halvfarryggen, the derived values for $\Theta$ are similar for both shelves (Table 3). Despite the similar stress reduction through thinning or removal of the ice shelf, increase of absolute flux across the grounding line differs. This asymmetry is not induced by asymmetric buttressing, but is caused by the difference in initial flux across the grounding line, which is almost an order of magnitude higher in the east than the counterpart in the west. If now the stress is reduced by the same ~~finite amount~~percentage, the flux imbalance between east and west will widen (Table 3), resulting in the divide ~~to migrate to~~ migrating to the west. We infer from our model simulations that while buttressing induces divide migration, it is by no means necessary to have asymmetric buttressing for the divide to migrate. The more important determining factor as to how far the divide is going to migrate is the absolute flux imbalance between the two sides of the divide. If we use the flux imbalance from the three different shelf thinning/removal simulations (Runs ~~8-10,~~8,10-11, Table 2), the relationship is almost linear between flux imbalance and the resulting divide migration. If this linear fit equation and the

modelled flux imbalances are used to predict divide migration for the same three simulations, migration amplitudes of -718 m, -277 m, and -16 m are predicted. This compares reasonably well with the computed divide migration amplitudes after 100 years of -734 m, -235 m, and -43 m, respectively. This does not mean that this relationship must be linear, but underlines the fact that flux imbalance is much more important than the buttressing provided by the ice shelf for divide migration.

**Table 3.** Flux calculations, derived buttressing factors, and stress reduction calculations for both sides of the divide for Halvfarryggen ice rise from Runs ~~8-10~~ 8,10-11 (Table 2). GL flux reduction in relation to the shelf thickness perturbation simulations (column 2) is computed by dividing ~~the~~ ΔGL Flux (column 3) by GL Flux (column 2) and the buttressing factor and stress reduction are calculated from Schoof (2007) (eq. 29).

| Simulation | GL reference flux at Year 0 [$\times 10^8$ m$^3$yr$^{-1}$] | GL flux at Year 0 [$\times 10^8$ m$^3$yr$^{-1}$] | ΔGL flux at Year 0 [$\times 10^8$ m$^3$yr$^{-1}$] | GL flux reduction [-] | Derived buttressing factor Θ [-] | Stress reduction [%] |
|---|---|---|---|---|---|---|
| No shelf east | 9.553 | 23.65 | ~~14.01~~ 14.10 | 0.592 | 0.21 | 79.0 |
| No shelf west | 1.874 | 5.227 | ~~3.354~~ 3.353 | 0.642 | 0.18 | 81.0 |
| 50% shelf east | 9.553 | 15.21 | 5.657 | 0.372 | 0.36 | 64.0 |
| 50% shelf west | 1.874 | 2.957 | 1.083 | 0.366 | 0.36 | 64.0 |
| 90% shelf east | 9.553 | 10.96 | 1.407 | 0.128 | 0.60 | 40.0 |
| 90% shelf west | 1.874 | 2.315 | 0.441 | 0.191 | 0.52 | 48.0 |

### 5.4 Comparison SMB and ocean induced divide migration

Despite the fact that the SMB perturbation represents the more physically realistic perturbation than the most extreme shelf thickness perturbation (shelf removal), the SMB perturbation results in fast divide migration and the shelf thickness perturbation leads to slow divide migration. This ~~has different consequences for the~~ leads us to different interpretation for the resulting geometry of the Raymond stack, with ~~fast migration~~ SMB perturbations leading likely to a Raymond stack abandoning and ~~slow migration~~ ocean perturbations resulting in a left tilted Raymond stack (Figure 2e,f).

The response of the divide position to ocean perturbations is primarily controlled by the subglacial topography with lateral buttressing only being a controlling factor of second order. The modelled short-lived response of the increased grounding-line flux to all ocean perturbations is typical of drainage basins located on prograde sloping bedrock (Figure 12), where the instantaneous removal of all buttressing leads to a sudden, but short-lived response. Similar results have been obtained from modelling of ice-shelf collapse in the Antarctic Peninsula region (Schannwell et al., 2018).

As both ice rises in the model domain, and to the authors' knowledge most other ice rises around Antarctica as well, are located on subglacial topography plateaus, the potential for grounding-line retreat is limited. Because ice flux across the grounding line is primarily a function of ice thickness at the grounding line (Schoof, 2007), the initial retreat of the grounding line on prograde

slopes often leads to thinner ice at the grounding line and in turn leads to a reduction of ice flux across the grounding line that can even be lower than before the perturbation. Similarly, the response of the divide position to SMB perturbations also seems to be primarily controlled by the subglacial topography with the magnitude of the flux imbalance between east and west of the divide being a controlling factor of secondary order. Evidence for this is provided by the unadjusted SMB perturbation (Run 5, Table 2) and the SMB grounding-line flux perturbation (Run 6, Table 2) simulations, which both converge to the same new steady-state divide position, even though the forcing is different by a factor of two.

As SMB perturbations directly affect surface topography, this type of perturbation leads to quicker response times of ice-divide migration in comparison with shelf thickness perturbation with e-folding times of 95-170 years and 30-50 years for shelf thickness and SMB simulations, respectively. This means that not only is the magnitude lower, but also the timing of ice-rise divide migration is delayed in the case of shelf thickness perturbations. Moreover, even though the magnitude of the initial perturbation is lower for the SMB simulations, divide migration is larger by a factor ~3.4 and ~3.9 for Halvfarryggen and Söråsen, respectively. The divide-migration rate and amplitude for SMB perturbations is most likely heavily dependent on the spatial pattern of the perturbation, with SMB perturbations near the divide likely leading to faster and larger divide migration than SMB perturbations that have their maximum farther away from the divide (Hindmarsh, 1996).

~~However, the~~

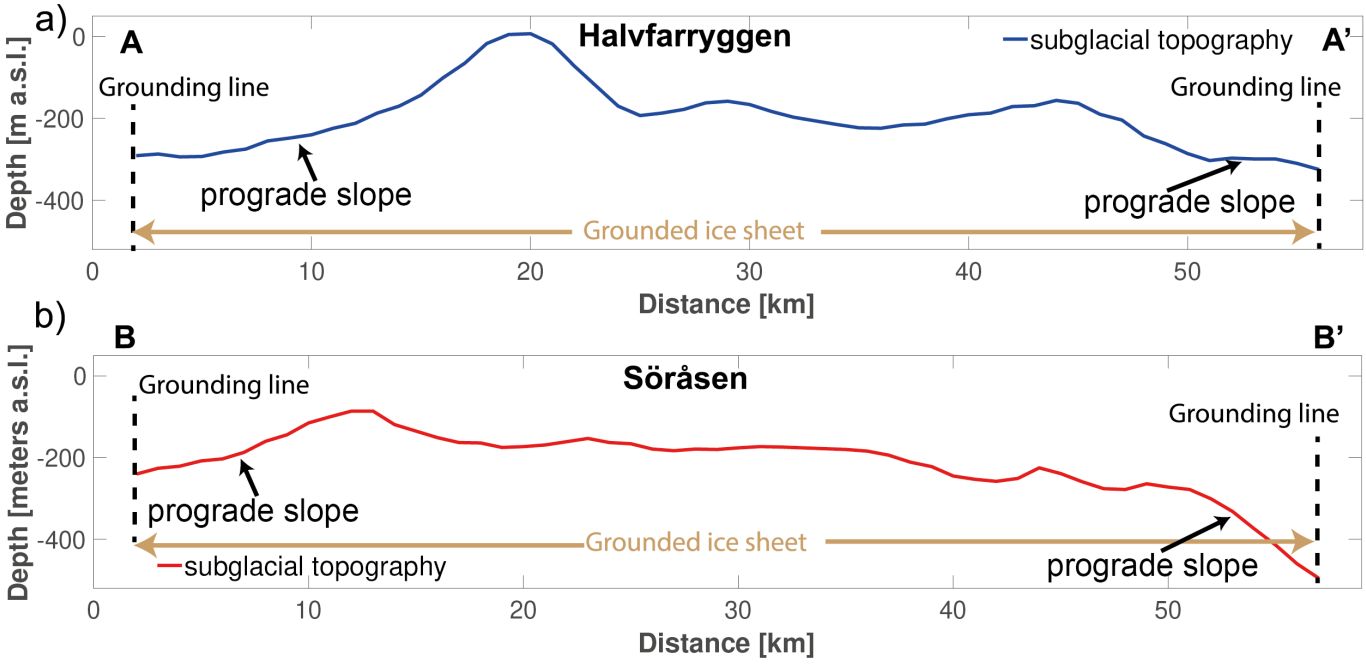


**Figure 12.** Cross sections of grounded subglacial topography from BEDMAP2 dataset (Fretwell et al., 2013) for Halvfarryggen (a) and Söråsen (b) ice rises, underlining the prograde sloping subglacial topography of both ice rises in the vicinity of the current grouning line.

In spite of the lower divide-migration rates computed ~~for Halvfarryggen and Söråsen~~ from shelf thickness perturbations~~are still important for the analysis of the~~ , the magnitude of the migration is still large enough to affect the geometry of Raymond stacks. The computed magnitudes are of similar amplitude to divide migration rates inferred for Siple Dome (Nereson and Waddington, 2002). Moreover, Ekström Ice Shelf and Jelbart Ice Shelf belong to the smaller ice shelves around Antarctica, making it likely that ice rises with larger ice flux across the grounding line in combination with larger buttressing provided by the surrounding ice shelves may well ~~cause~~ have the potential to experience larger divide migration rates.

The rate of triple junction migration appears to be closely linked to the migration rate of the main divide arm and thus seems to be similarly susceptible to migration ~~than~~ as divide ridges. ~~This~~ There appears to be a widening/splitting trend of the triple junction in the SMB simulations and a narrowing/merging trend for the shelf thickness simulations. However, the migration amplitudes are insufficient to evaluate if a merging or splitting of a divide triple junction might explain observed radar features such as relic arches in the divide flank (Drews et al., 2015). Migration of the triple junction also bears importance for selecting potential ice-core drilling sites on these type of ice domes and a tilted Raymond stack may indicate a displacement of the triple junction as well.

### 5.5 Model limitations

By calibrating our ice-sheet model on the Ekström Ice Shelf catchment, we aim to introduce commonly employed initialisation techniques in large-scale ice-sheet modelling to ice-rise modelling. The advantage of the calibration is that buttressing is simulated in a realistic fashion. Without the calibration, large thinning/thickening rates would result in unrealistic model results. However, the calibration matches observed horizontal velocities with modelled horizontal velocities without any constraints on vertical ice velocities. This leads to the situation that any errors in the horizontal velocities propagate into the vertical velocity through mass conservation. As horizontal velocities in the divide region are close to zero, small errors in horizontal velocities have a large effect on vertical velocities and ~~thus the reconstruction of Raymond stacks~~therefore we were unable to solve for the age field (Raymond stacks). In addition, due to computational constraints, only 10 equally spaced vertical layers could be employed. For an ice thickness of ∼900 m at Halvfarryggen ice rise, this corresponds to a vertical resolution of ∼90 meters. While this vertical resolution is sufficient for our ice-rise divide migration purposes, a much higher vertical resolution (∼30-40 layers) would be necessary to model Raymond arches at the required detail (Drews et al., 2015). Similarly, despite refining the mesh locally down to ~~300~~350 m, ~~we do not observe first order convergence in the ice-divide migration amplitude as we refine the mesh. This means that that the difference between migration amplitudes at 1 km and 0.5 km horizontal resolution should be half of the difference between 2 km and 1 km. While this does not affect the results of the paper, it indicates that even higher mesh resolutions ought to be employed and that~~ this may still not suffice for some of the shelf removal simulations, where finer meshes than presented here (<~~300~~350 m) may result in larger divide migration amplitudes.

In spite of the advanced ice-sheet model employed, compromises in the complexity of the experimental setup had to be made to make these simulations computationally feasible. These simplifications or approximations were done with the goal of focussing on ice-rise divide migration at the expense of accurately simulating Raymond arch formation. In the following, we will list these simplifications and regard each of them as future avenues to improve on the simulations presented here. As suggested

by many previous ice-rise divide studies, the commonly used exponent of the ice rheology law (n=3) is not able to reproduce the Raymond arch amplitudes from observations, but often a higher exponent (~~n~~n≈4.5) is chosen that better matches the arch amplitudes from observations (Martín et al., 2014; Drews et al., 2015; Bons et al., 2018). Moreover, Martín et al. (2009a) showed that the commonly employed approximation of ice being an isotropic material in large-scale ice-sheet models is not valid at ice divides, where a preferential orientation of the ice crystals leads to enhanced ice deformation. Changes in ice deformation can also be caused by changes in ice temperature, where warmer ice leads to enhanced ice deformation and cold ice reduces ice deformation. While the effect of temperature and enhanced/decreased ice deformation could introduce differences in divide position, to the author's knowledge no one has comprehensively shown this. However, previous studies have found that thermomechanically coupled models exhibit warmer ice at the base under the divide (Martín and Gudmundsson, 2012), which could potentially indicate that divide migration may occur faster. As our model is not thermomechanically coupled, these effects are ignored in the simulations. Even though ice temperature and anisotropy have been identified as important parameters to be able to reproduce the internal structure of ice divides, it is still uncertain as to how much they affect divide migration.

We performed our simulations with only one type of sliding law (linear Weertmann), without testing alternative implementations. Even though other modelling studies have shown that this type of sliding law generally results in smaller grounding-line retreat than other sliding laws (e.g. pressure-limited sliding law; (e.g. Schannwell et al., 2018)), it remains difficult to assess the importance of the sliding law for divide migration. On the one hand, reduced basal drag may lead to enhanced grounding-line retreat (Price et al., 2008; Gillet-Chaulet et al., 2016), but on the other hand ice near the divide region might be frozen to the bed and sliding can be neglected in these areas. Therefore, we believe that the choice of the sliding law is likely to have a limited impact on our results. Given that many previous ice divide modelling studies assume no basal sliding at all (e.g. Martín et al., 2006), the largest impact of this simplification will be on the grounding-line position in the ocean perturbation simulations. But even there, owing to the prograde sloping subglacial topography, the effect of different sliding laws should not be a major concern for the computed divide migration rates.

## 6 Conclusions

We used a calibrated 3D ice-sheet model including grounding-line dynamics and shelf flow for the Ekström catchment to investigate the coupled transient response of ice-rise divides and triple junctions to perturbations in the SMB and ice-shelf thickness. Our perturbation simulations for the Ekström catchment reveal that SMB perturbations result in fast divide migration (up to 3.5 m/yr), while shelf thickness perturbations only trigger slow divide migration (<0.75 m/yr). The amplitude of divide migration is predominately controlled by the subglacial topography and SMB with ice-shelf buttressing being of secondary importance.

We find in our simulations that asymmetric buttressing is not a required condition for ice-rise divide migration, but rather ~~as to~~ how much the divide will migrate is determined by the flux imbalance between either side of the divide. Both ice rises show a closely coupled response to the perturbations with divide migration being similar in timing and magnitude. Based

on our simulations, the geometry of the Raymond stack could provide clues about the forcing mechanism behind the divide migration, with an abandoned Raymond stack being more likely linked to SMB perturbations. For tilted Raymond stacks ~~,~~ the interpretation of the internal structure remains difficult with either a smaller SMB perturbation than prescribed here or shelf thickness perturbations ~~are~~ equally likely. ~~This separation of the~~ It is integral to further unravel (e.g. through synthetic experiments) the different trigger mechanisms for different types of Raymond Arch geometries ~~is integral~~ in order to fully unlock the potential of ice rises as ice-dynamic archives, potential ice-core drilling site, and to better constrain paleo ice-sheet models.

We find that a high mesh resolution (<500 m) is required in the vicinity of the dome and the grounding-line to capture ice-rise divide migration at the desired detail, as mean maximum migration amplitude is <4 km in our perturbation experiments. To avoid unrealistic ice mass loss in transient simulations around the divide region, where longitudinal and bridging stresses are important, the same force balance approximation (e.g. FS for ice divides) should be used in the initialisation and forward simulation of the ice-sheet model.

Finally, migration of the triple junction closely follows the migration pattern of the main ridge, which may ~~proof~~ prove useful in the future selection of ice-core drilling sites. ~~For example, in the absence of divide migration records, the migration history of the triple junction could be used as proxy to locate the best ice-core drilling site~~However, more targeted simulations are required to determine whether a merging or splitting of the triple junction can explain relic Raymond stacks in the flank of ice rises. The model setup is suitable for glacial/interglacial simulations on the catchment scale, providing the next step forward to unravel the ice-dynamic history stored in ice rises all around Antarctica.

*Author contributions.* CS and RD conceived the study with input from OE, TE, and CM. Simulations were run by CS with assistance from FGC. The manuscript was written by CS and RD and all authors contributed to editing and revision.

*Competing interests.* The authors declare that there are no competing interests

*Acknowledgements.* We thank V. Helm for providing us with the TanDEM-X digital elevation models. CS was supported by the Deutsche Forschungsgemeinschaft (DFG) grant EH329/11-1 (to TAE) in the framework of the priority programme "Antarctic Research with comparative investigations in Arctic ice areas"~~by the grant MA 3347/10-1~~. The authors gratefully acknowledge the compute and data resources provided by the Leibniz Supercomputing Centre (www.lrz.de).

## References


Arndt, J. E., Schenke, H. W., Jakobsson, M., Nitsche, F. O., Buys, G., Goleby, B., Rebesco, M., Bohoyo, F., Hong, J., Black, J., Greku, R., Udintsev, G., Barrios, F., Reynoso-Peralta, W., Taisei, M., and Wigley, R.: The International Bathymetric Chart of the Southern Ocean (IBCSO) Version 1.0-A new bathymetric compilation covering circum-Antarctic waters: IBCSO VERSION 1.0, Geophysical Research Letters, 40, 3111–3117, https://doi.org/10.1002/grl.50413, 2013.

Bons, P. D., Kleiner, T., Llorens, M.-G., Prior, D. J., Sachau, T., Weikusat, I., and Jansen, D.: Greenland Ice Sheet: Higher nonlinearity of ice flow significantly reduces estimated basal motion, Geophysical Research Letters, 45, 6542–6548, https://doi.org/10.1029/2018GL078356, 2018.

Brook, E. J., Wolff, E., Dahl-Jensen, D., Fischer, H., and Steig, E. J.: The future of ice coring: international partnerships in ice core sciences (IPICS), PAGES news, 14, 6–10, 2006.

Callens, D., Drews, R., Witrant, E., Philippe, M., and Pattyn, F.: Temporally stable surface mass balance asymmetry across an ice rise derived from radar internal reflection horizons through inverse modeling, Journal of Glaciology, pp. 1–10, https://doi.org/10.1017/jog.2016.41, 2016.

Conway, H. and Rasmussen, L. A.: Recent thinning and migration of the Western Divide, central West Antarctica, Geophysical Research Letters, 36, L12 502, https://doi.org/10.1029/2009GL038072, 2009.

Conway, H., Hall, B. L., Denton, G. H., Gades, A. M., and Waddington, E. D.: Past and Future Grounding-Line Retreat of the West Antarctic Ice Sheet, Science, 286, 280, https://doi.org/10.1126/science.286.5438.280, 1999.

Cornford, S. L., Martin, D. F., Payne, A. J., Ng, E. G., Le Brocq, A. M., Gladstone, R. M., Edwards, T. L., Shannon, S. R., Agosta, C., van den Broeke, M. R., Hellmer, H. H., Krinner, G., Ligtenberg, S. R. M., Timmermann, R., and Vaughan, D. G.: Century-scale simulations of the response of the West Antarctic Ice Sheet to a warming climate, The Cryosphere, 9, 1579–1600, https://doi.org/10.5194/tc-9-1579-2015, 2015.

Drews, R., Martín, C., Steinhage, D., and Eisen, O.: Characterizing the glaciological conditions at Halvfarryggen ice dome, Dronning Maud Land, Antarctica, Journal of Glaciology, 59, 9–20, https://doi.org/10.3189/2013JoG12J134, 2013.

Drews, R., Matsuoka, K., Martín, C., Callens, D., Bergeot, N., and Pattyn, F.: Evolution of Derwael Ice Rise in Dronning Maud Land, Antarctica, over the last millennia, Journal of Geophysical Research: Earth Surface, 120, 564–579, https://doi.org/10.1002/2014JF003246, 2015.

Favier, L., Pattyn, F., Berger, S., and Drews, R.: Dynamic influence of pinning points on marine ice-sheet stability: a numerical study in Dronning Maud Land, East Antarctica, The Cryosphere, 10, 2623–2635, https://doi.org/10.5194/tc-10-2623-2016, 2016.

Fretwell, P., Pritchard, H. D., Vaughan, D. G., Bamber, J. L., Barrand, N. E., Bell, R., Bianchi, C., Bingham, R. G., Blankenship, D. D., Casassa, G., Catania, G., Callens, D., Conway, H., Cook, A. J., Corr, H. F. J., Damaske, D., Damm, V., Ferraccioli, F., Forsberg, R., Fujita, S., Gim, Y., Gogineni, P., Griggs, J. A., Hindmarsh, R. C. A., Holmlund, P., Holt, J. W., Jacobel, R. W., Jenkins, A., Jokat, W., Jordan, T., King, E. C., Kohler, J., Krabill, W., Riger-Kusk, M., Langley, K. A., Leitchenkov, G., Leuschen, C., Luyendyk, B. P., Matsuoka, K., Mouginot, J., Nitsche, F. O., Nogi, Y., Nost, O. A., Popov, S. V., Rignot, E., Rippin, D. M., Rivera, A., Roberts, J., Ross, N., Siegert, M. J., Smith, A. M., Steinhage, D., Studinger, M., Sun, B., Tinto, B. K., Welch, B. C., Wilson, D., Young, D. A., Xiangbin, C., and Zirizzotti, A.: Bedmap2: improved ice bed, surface and thickness datasets for Antarctica, The Cryosphere, 7, 375–393, https://doi.org/10.5194/tc-7-375-2013, 2013.

Fürst, J. J., Durand, G., Gillet-Chaulet, F., Merino, N., Tavard, L., Mouginot, J., Gourmelen, N., and Gagliardini, O.: Assimilation of Antarctic velocity observations provides evidence for uncharted pinning points, The Cryosphere, 9, 1427–1443, https://doi.org/10.5194/tc-9-1427-2015, 2015.

Gagliardini, O., Zwinger, T., Gillet-Chaulet, F., Durand, G., Favier, L., de Fleurian, B., Greve, R., Malinen, M., Martín, C., Råback, P., Ruokolainen, J., Sacchettini, M., Schäfer, M., Seddik, H., and Thies, J.: Capabilities and performance of Elmer/Ice, a new-generation ice sheet model, Geosci. Model Dev., 6, 1299–1318, https://doi.org/10.5194/gmd-6-1299-2013, 2013.

Gillet-Chaulet, F. and Hindmarsh, R. C. A.: Flow at ice-divide triple junctions: 1. Three-dimensional full-Stokes modeling: Ice-divide triple junction modeling, Journal of Geophysical Research: Earth Surface, 116, F02 023, https://doi.org/10.1029/2009JF001611, 2011.

Gillet-Chaulet, F., Hindmarsh, R. C. A., Corr, H. F. J., King, E. C., and Jenkins, A.: *In-situ* quantification of ice rheology and direct measurement of the Raymond Effect at Summit, Greenland using a phase-sensitive radar, Geophysical Research Letters, 38, L24 503, https://doi.org/10.1029/2011GL049843, 2011.

Gillet-Chaulet, F., Gagliardini, O., Seddik, H., Nodet, M., Durand, G., Ritz, C., Zwinger, T., Greve, R., and Vaughan, D. G.: Greenland ice sheet contribution to sea-level rise from a new-generation ice-sheet model, The Cryosphere, 6, 1561–1576, https://doi.org/10.5194/tc-6-1561-2012, 2012.

Gillet-Chaulet, F., Durand, G., Gagliardini, O., Mosbeux, C., Mouginot, J., Rémy, F., and Ritz, C.: Assimilation of surface velocities acquired between 1996 and 2010 to constrain the form of the basal friction law under Pine Island Glacier, Geophysical Research Letters, 43, 10,311–10,321, https://doi.org/10.1002/2016GL069937, 2016.

Goel, V., Brown, J., and Matsuoka, K.: Glaciological settings and recent mass balance of Blåskimen Island in Dronning Maud Land, Antarctica, The Cryosphere, 11, 2883–2896, https://doi.org/10.5194/tc-11-2883-2017, 2017.

Hindmarsh, R. G. A.: Stochastic perturbation of divide position, Annals of Glaciology, 23, 94–104, https://doi.org/10.3189/S0260305500013306, 1996.

Hofstede, C., Eisen, O., Diez, A., Jansen, D., Kristoffersen, Y., Lambrecht, A., and Mayer, C.: Investigating englacial reflections with vibro- and explosive-seismic surveys at Halvfarryggen ice dome, Antarctica, Annals of Glaciology, 54, 189–200, https://doi.org/10.3189/2013AoG64A064, 2013.

Jacobson, H. P. and Waddington, E. D.: Recumbent folding of divide arches in response to unsteady ice-divide migration, Journal of Glaciology, 51, 201–209, 2005.

Jezek, K. and 5 RAMP-Product-Team:: RAMP AMM-1 SAR Image Mosaic of Antarctica, Alaska Satellite Facility, in association with the National Snow and Ice Data Center, 2002.

Kingslake, J., Martín, C., Arthern, R. J., Corr, H. F. J., and King, E. C.: Ice-flow reorganization in West Antarctica 2.5 kyr ago dated using radar-derived englacial flow velocities, Geophysical Research Letters, 43, 9103–9112, https://doi.org/10.1002/2016GL070278, 2016.

Lenaerts, J. T., Brown, J., Van Den Broeke, M. R., Matsuoka, K., Drews, R., Callens, D., Philippe, M., Gorodetskaya, I. V., Van Meijgaard, E., Reijmer, C. H., Pattyn, F., and Van Lipzig, N. P.: High variability of climate and surface mass balance induced by Antarctic ice rises, Journal of Glaciology, 60, 1101–1110, https://doi.org/10.3189/2014JoG14J040, 2014.

MacAyeal, D. R.: A tutorial on the use of control methods in ice-sheet modeling, Journal of Glaciology, 39, 91–98, https://doi.org/10.3189/S0022143000015744, 1993.

Martín, C. and Gudmundsson, G. H.: Effects of nonlinear rheology, temperature and anisotropy on the relationship between age and depth at ice divides, The Cryosphere Discussions, 6, 2221–2245, https://doi.org/10.5194/tcd-6-2221-2012, 2012.

Martín, C., Hindmarsh, R. C. A., and Navarro, F. J.: Dating ice flow change near the flow divide at Roosevelt Island, Antarctica, by using a thermomechanical model to predict radar stratigraphy, Journal of Geophysical Research, 111, F01 011, https://doi.org/10.1029/2005JF000326, 2006.

Martín, C., Gudmundsson, G. H., Pritchard, H. D., and Gagliardini, O.: On the effects of anisotropic rheology on ice flow, internal structure, and the age-depth relationship at ice divides, Journal of Geophysical Research, 114, F04 001, https://doi.org/10.1029/2008JF001204, 2009a.

Martín, C., Hindmarsh, R. C. A., and Navarro, F. J.: On the effects of divide migration, along-ridge flow, and basal sliding on isochrones near an ice divide, Journal of Geophysical Research, 114, F02 006, https://doi.org/10.1029/2008JF001025, 2009b.

Martín, C., Gudmundsson, G. H., and King, E. C.: Modelling of Kealey Ice Rise, Antarctica, reveals stable ice-flow conditions in East Ellsworth Land over millennia, Journal of Glaciology, 60, 139–146, https://doi.org/10.3189/2014JoG13J089, 2014.

Matsuoka, K., Hindmarsh, R. C., Moholdt, G., Bentley, M. J., Pritchard, H. D., Brown, J., Conway, H., Drews, R., Durand, G., Goldberg, D., Hattermann, T., Kingslake, J., Lenaerts, J. T., Martín, C., Mulvaney, R., Nicholls, K. W., Pattyn, F., Ross, N., Scambos, T., and Whitehouse, P. L.: Antarctic ice rises and rumples: Their properties and significance for ice-sheet dynamics and evolution, Earth-Science Reviews, 150, 724–745, https://doi.org/10.1016/j.earscirev.2015.09.004, 2015.

Morland, L. W.: Unconfined Ice-Shelf Flow, in: Dynamics of the West Antarctic Ice Sheet, edited by Van der Veen, C. J. and Oerlemans, J., vol. 4, pp. 99–116, Springer Netherlands, Dordrecht, https://doi.org/10.1007/978-94-009-3745-1_6, 1987.

Neckel, N., Drews, R., Rack, W., and Steinhage, D.: Basal melting at the Ekström Ice Shelf, Antarctica, estimated from mass flux divergence, Annals of Glaciology, 53, 294–302, https://doi.org/10.3189/2012AoG60A167, 2012.

Nereson, N. A. and Waddington, E. D.: Isochrones and isotherms beneath migrating ice divides, Journal of Glaciology, 48, 95–108, 2002.

Nereson, N. A., Raymond, C. F., Waddington, E. D., and Jacobel, R. W.: Migration of the Siple Dome ice divide, West Antarctica, Journal of Glaciology, 44, 643–652, https://doi.org/10.3189/S0022143000002148, 1998.

Pettit, E. C., Thorsteinsson, T., Jacobson, H. P., and Waddington, E. D.: The role of crystal fabric in flow near an ice divide, Journal of Glaciology, 53, 277–288, https://doi.org/10.3189/172756507782202766, 2007.

Price, S. F., Conway, H., Waddington, E. D., and Bindschadler, R. A.: Model investigations of inland migration of fast-flowing outlet glaciers and ice streams, Journal of Glaciology, 54, 49–60, https://doi.org/10.3189/002214308784409143, 2008.

Raymond, C. F.: Deformation in the vicinity of ice divides, Journal of Glaciology, 29, 357–373, https://doi.org/10.1017/S0022143000030288, 1983.

Rignot, E., Mouginot, J., and Scheuchl, B.: Ice Flow of the Antarctic Ice Sheet, Science, 333, 1427–1430, https://doi.org/10.1126/science.1208336, 2011.

Schannwell, C., Cornford, S., Pollard, D., and Barrand, N. E.: Dynamic response of Antarctic Peninsula Ice Sheet to potential collapse of Larsen C and George VI ice shelves, The Cryosphere, 12, 2307–2326, https://doi.org/10.5194/tc-12-2307-2018, 2018.

Schoof, C.: Ice sheet grounding line dynamics: Steady states, stability, and hysteresis, Journal of Geophysical Research, 112, F03S28, https://doi.org/10.1029/2006JF000664, 2007.